The development of two novel interhemispheric transfer time tasks and application within a pilot paediatric moderate-severe traumatic brain injury cohort

By Kelly Kordom | KRDKEL001

In fulfilment of the requirements for the degree of Master of Science in Neuroscience (surgery)

Division of Paediatric Neurosurgery
Department of Surgery
Faculty of Health Sciences
UNIVERSITY OF CAPE TOWN

Supervisor: Professor Anthony Figaji

Submission: October, 2023

Declaration

I, **KELLY KORDOM**, hereby declare that the work on which this dissertation/thesis is based is my original work (except where acknowledgements indicate otherwise) and that neither the whole work nor any part of it has been, is being, or is to be submitted for another degree in this or any other university.

I empower the university to reproduce, for the purpose of research, either the whole or any portion of the contents in any manner whatsoever.

Name: Kelly Kordom

Signature: Signed by candidate

Date: 24 October 2023

Acknowledgements

Firstly, I would like to thank God who is forever faithful, has blessed me tremendously and carried me throughout this journey.

Thank you to the National Research Foundation and my parents for funding my studies.

A special thank you to my supervisor Professor Anthony Figaji. Your constant reminder of why this research is important truly kept me going. What I have gained through being part of the African Brain Child group is immeasurable, and I am beyond grateful for the opportunity to be part of the ABC family.

Dr. Sarah McFie-Shwartz, I will never forget the mentorship you provided during the very early stages of this research. Even under some very difficult circumstances you went above and beyond to guide me to the best of your abilities. Your patience and passion for the project motivated me to continue pursuing the full potential of this project.

My parents went through every effort to provide me with the opportunities to pursue the best version myself. I especially would like to thank my mother for always praying for me, for always encouraging me and my father who was truly part of every step of this thesis. Thank you to my two younger brothers for always cheering me on along the side-lines. I love you both dearly.

Lastly, this project would not have been possible without all the volunteers and patients who participated in the study. I am so thankful for every single person who took time from their busy lives to contribute to this research.

Abstract

Introduction: Children are particularly vulnerable to injuries sustained during and following moderate or severe traumatic brain injury (TBI) as it can interrupt normal childhood development. Our ability to assess functional outcomes in the post-acute phase of injury is still limited, but imperative for appropriate prognosis and allocation of resources for rehabilitation. Advanced MRI techniques such as diffuse tensor imaging have shown that moderate-severe TBI often results in compromised white matter integrity and has been associated with poor neurocognitive outcomes in children. The corpus callosum is the main commissural region of the brain and one of the most widely reported regions of injury during TBI. Interhemispheric transfer time (IHTT) has therefore been suggested to assess the functional integrity of the corpus callosum.

Aim: In this study we aimed to explore the development of two novel electroencephalogram (EEG) based IHTT tasks by investigating the reliability of the measured IHTTs and their feasibility for use in young children who had sustained a TBI.

Methods: Two IHTT tasks were developed on MATLAB; a simple motor task and a non-motor task. Both tasks consisted of checkerboard visual stimuli presentation to evoke visual event related potentials (ERPS) on an EEG recording. An adult cohort was recruited to perform these two tasks on a laptop while an EEG was recorded to ascertain if the tasks were effective in producing visual ERPs, and to assess the test-retest and interrater reliability of the two tasks. Reliability was assess using the Intraclass Correlation Coefficient (ICC). Once assessment was complete in the adult cohort, six paediatric moderate-severe TBI patients were recruited to evaluate if the tasks were feasible and appropriate for a young paediatric TBI cohort. Similarly, they were required to perform both the motor and non-motor IHTT tasks on a laptop while an EEG was recorded. IHTTs for both cohorts were measured by calculating latencies of ERP components.

Results: All adult participants were able to carry out the tasks with minimal difficulty. The EEG recordings show that the tasks effectively produced ERPs at the occipital and parietal sites. For IHTTs measured from the occipital sites, the calculated IHTTs provided high test-retest reliability for the motor task and moderate test-retest reliability for the non-motor task. Overall moderate inter-rater reliability between the motor and non-motor tasks was also calculated for IHTT measured at the occipital sites. All ICC test-retest and inter-rater reliability values for the IHTT calculated from the parietal sites were considerably low. In our paediatric TBI cohort all

participants were able to complete both tasks, however IHTT could not be calculated from the motor task in 50% of the patients due to excessive movement. IHTT could be measured from the non-motor tasks for all patients.

Conclusions: The high test-retest reliability for the motor tasks indicates that the IHTT measures are reproducible and independent of the task and EEG set-up. The moderate reliability values for the non-motor tasks are promising and also suggests that further investigation is required to assess what test conditions could improve the ICC scores of the non-motor tasks. The non-motor task served as a better option to calculated IHTT in the paediatric TBI cohort, and indicates that the current motor task may still not be simple enough for the young paediatric TBI population. The non-motor task seems to be a promising tool to measure IHTT in young patients, especially in individuals with cognitive, physical and behavioural limitations following TBI.

TABLE OF CONTENTS

Declaration ii
Acknowledgements iii
Abstract iv
Abbreviations ix
LIST OF FIGURES xi
LIST OF TABLES xiii
Chapter 1: Introduction 1
1.1 Overview 1
1.2 Clinical significance of the study 2
1.3 Research Statement 3
Chapter 2: Literature Review 4
2.1 Traumatic Brain Injury 4
2.1.1 Overview 4
2.1.2 Primary mechanisms of Injury 4
2.1.3 Diffuse axonal injury 5
2.1.4 Secondary mechanisms of injury 6
2.2 Outcome and predictors of functional recovery following paediatric traumatic brain injury. 9
2.2.1 Outcomes of traumatic brain injury 9
2.2.2 Predictors of Outcome 9
2.3 The use of neuroimaging in TBI 11
2.3.1 Neuroimaging in the acute phase of TBI 11
2.3.2 Diffuse Tensor Imaging 12
2.3.3 Magnetic resonance spectrometry 13
2.3.4 Limitations of advanced neuroimaging 15
2.4 The corpus callosum 16
2.4.1 Corpus callosum anatomy and function 16
2.4.2 Damage to the corpus callosum following TBI 17
2.5 Interhemispheric Transfer time 18
2.5.1 Neural wiring of the visual system 18
2.5.2 Early studies of interhemispheric transfer time 19
2.5.3 Electrophysiological measures of IHTT 21
2.5.4 IHTT measures in pTBI cohorts 22

2.6: Aims and Objectives 28
2.6.1 Aim 28
2.6.2 Objectives 28
Chapter 3: Methodology 29
3.1 Development of the IHTT Tasks 29
3.1.1 Overview 29
3.1.2 Display and Duration Settings of Task Components 30
3.1.3 The motor task 32
3.1.4 Non-motor Task 33
3.1.5 Output Data from MATLAB 35
3.2 EEG Recording 36
3.3 Interface between MATLAB presentation laptop and BIOPAC EEG 37
3.4 EEG Pre-processing 38
3.5 IHTT Calculation 38
3.6 Statistical Analysis 39
3.7 Participants and IHTT Task Testing Procedure 40
3.7.1 Adult cohort for test-retest reliability analysis 40
3.7.2 Adult cohort testing procedure 40
3.7.3 Paediatric Cohort 41
3.7.4 Paediatric TBI cohort testing procedure 42
Chapter 4: Results 43
4.1 Feasibility reports for adult test-retest cohort 43
4.2 Identification of ERPs and IHTT calculation 45
4.3 Test-retest and interrater reliability 48
4.5 Observational reports on feasibility for paediatric cohort 49
4.6 Number of incorrect scores for pTBI cohort 49
4.7 Identification of ERPs and IHTT calculation for pTBI cohort 49
Chapter 5: Discussion 52
5.1 Feasibility and ERP of IHTT tasks in adult cohort 52
5.2 Parietal vs occipital measures of interhemispheric transfer time 53
5.3 Test-retest and interrater reliability of IHTT measures 54
5.4 EEG IHTT measures compared with previous studies 55
5.5 Detection of asymmetries in IHTT 55

5.6 Feasibility reports in children 56
5.6.1 Difficulties with assessment in the motor task 56
5.6.2 Feasibility and ERP detection in non-motor tasks 57
5.7 Comparison of IHTT values to other pTBI cohorts and adults 57
5.8 pTBI in the South African context 58
5.9 Limitations 59
5.9.1 Lack of objective measure for attention in non-motor task 59
5.9.2 Low number of trials for ERP averaging 59
5.9.3 Homogenous adult and pTBI cohorts 60
5.10 Future Research 60
Chapter 6: Final Conclusions 62
References 63

Abbreviations

ATP	adenosine triphosphate
CC	corpus callosum
Cho	Choline
CT	computed tomography
DAI	diffuse axonal injury
DTI	diffusion tensor imaging
DWI	diffusion weight imaging
ECG	electrocardiogram
EEG	electroencephalogram
EOG	electrooculogram
ERP	event related potential
FA	fractional anisotropy
FHS	Faculty of Health Sciences
GCS	Glasgow Coma Scale
HREC	Human Research Ethics Committee
ICC	Intraclass Correlation Coefficient
ICP	intracranial pressure
IHTT	interhemispheric transfer time
LVF	left visual field
MRI	magnetic resonance imaging
MRS	magnetic resonance spectroscopy
MVA	motor vehicle accident
NAA	N-acetyl aspartate
TBI	traumatic brain injury
pTBI	paediatric traumatic brain injury
RCWMCH	Red Cross War Memorial Children's Hospital
RVF	right visual field
SES	socioeconomic status
SNR	signal to noise ratio

UCLA	University of California, Los Angeles
UCT	University of Cape Town
WM	white matter

LIST OF FIGURES

Figure 1**:** Pathophysiology of TBI; the diagram above aims to depict the pathophysiology of TBI from the moment of impact. The primary insults are depicted in blue including contusion, brain haemorrhage and diffuse axonal injury. These injuries result from the direct injury to the brain parenchyma and almost instantaneously. All these contribute to the secondary insults that are depicted in orange. The diagram shows that ICP arise from multiple origins including the breakdown of the BBB, brain swelling and bleeding, where prolonged raised ICP is generally associated with poorer outcomes because patients are at higher risk for ischaemia and brain herniation. While it may appear that these mechanisms occur in linear manner, usually they tend to occur simultaneously and may continue hours and days following the initial injury. 8
Figure 2: Sagittal section of the brain that slices through the midline locating the major regions of the CC. The rostrum is the most anterior portions of the CC that connects the orbital surfaces of the frontal lobes. The genu connects the medial and lateral surfaces of the frontal lobes. Posterior portions including the posterior midbody, isthmus and splenium are involved in transfer of somatosensory information and connects to the parietal, temporal and occipital lobes. 16
Figure 3: Schematic of the visual pathway from the eyes to the brain. Depiction of how all visual information from the RVF is first processed by the left hemisphere and vice versa for the information from LVF. 18
Figure 4: Overlapped averaged waveforms from parietal sites P3 and P4 displaying ERPs produced after visual stimulus onset. For RVF stimulation P3 electrode is the placed on the contralateral hemisphere and the P4 electrode is placed above the ipsilateral hemisphere. The most negative peak (N1) of the contralateral hemisphere appears before that of the ipsilateral hemisphere. The latency between the respective N1 peaks represents the IHTT (Chaumillion et al 2018). 22
Figure 5: Depiction of the participant task set-up. The script is designed so that the participant sits 46-50cm from the screen with the fixation point positioned at eye level. While the participant is completing the task an EEG is recorded simultaneously, as explained in chapter 3.2. 29
Figure 6: Lines 84-103 of the MATLAB script for the tasks that define the visual properties of the checkerboard, fixation point and letters displayed. The hashed out portions in green define the variables of the corresponding code. 30
Figure 7: Lines 50-59 of the MATLAB script that contains variables of the tasks that contributes to the durations of the fixation point, checkerboard, and letter presentation. These are further described in table 3. The “p.nTrails” variable also allowed one to enter how many trials will be displayed for a particular session. This number had to be an even number for equal number of trials for the LVF and RVF. 31
Figure 8: The two diagrams depict the timeline of sequence of events for the motor (A) and non-motor (B) tasks for each trial. Each trial is a duration of 5.5s for both tasks, however the motor tasks also consist of the letter presentation and beep that signals the participant to respond to the with the appropriate keyboard letter response. 34
Figure 9: An example of output data provided by MATLAB following completion of eight trials of the motor task. Each parameter is further described in table 5. The correct parameter was used for elimination of incorrect trials during the EEG preprocessing stage. 35
Figure 10: Experimental set up (A) Highlighted EEG electrodes of interest. The parietal sites (P3/P4) and occipital sites (O1/O2) are well described in their use for visual ERP visualisation.

P3 and O1 represent the left hemisphere and P2 and O2 represent the right hemisphere. (B) Experimental conditions for the LVF and RVF. All stimuli presented to the LVF will first project in the right (contralateral) hemisphere and then transfer to the left (ipsilateral) hemisphere via the CC. The ERP will occur first in the P4 and O2 electrodes and then in the P3 and O1 electrodes. Similarly, all stimuli presented to the RVF will first project to the left (contralateral) hemisphere and then transfer to the right (ipsilateral) hemisphere via the CC. The ERP will occur first in the P3 and O1 electrodes and then in the P4 and O2 electrodes. 36
Figure 11: (A) Pathway representing how information from the IHTT tasks and EEG recordings are combined. (B) EEG outputs once task was completed. The parietal and occipital electrode sites were of main interest, which is why those four are highlighted in the figure. The peaks in the last two digital input channels indicates when visual stimulus was presented during the task. Digital input channel 32 (blue) corresponds with stimuli displayed to the RVF and input channel 35 (red) corresponds with stimuli displayed to the LVF. 37
Figure 12: The above box plots displays the number of incorrect trials recorded by the motor tasks, as well as additional trials removed from the motor and non-motor tasks. The number for incorrect trials recorded for the adults were relatively low with a 98% correct response rate in the motor task. The plot also shows that while the correct response rate is high, additional trials still had to be removed due to excessive eye blinking or movement artefacts that could not be corrected for. 43
Figure 13: The two graphs depict ERPs produced by the occipital electrodes (O1 and O2) for visual stimuli presented to the RVF. The averaged graphs of the two electrodes were overlapped to visualise the latency between the N1 peaks – recognized as the largest negative peak of the ERP where a clear latency is visible. Graph (A) shows the ERPs produced by the motor task and graph (B) shows produced by the non-motor task. For both tasks the N1 peak appears about 340-350 milliseconds after the digital peak. 45
Figure 14: The two graphs depict ERPs produced by the parietal electrodes (P3 and P4) for visual stimuli presented to the RVF. Similarly, to figure 13 graph (A) shows the ERPs produced by the motor task and graph (B) shows produced by the non-motor task. For both tasks the N1 peak appears about 340-350 milliseconds after the digital peak. The N1 latency appears to be shorter, and variable compared to the occipital sites for both task; about 320 milliseconds for the motor task and 280 milliseconds for the non-motor task. 46
Figure 15: The two graphs represent averaged and overlapped O1-O2 channels for the digital inputs from the IHTT tasks performed by the pTBI cohort. The red graph represents the O1 channel, and the blue graph represents the O2 channel. (A) Overlapped occipital channels when the participant performed the motor task for the RVF. (B) Overlapped occipital electrode channels from the non-motor task for the LVF. 50
Figure 16: Study cohort for the pTBI patients – summary on task performance and IHTT calculations for the pTBI group. 51

LIST OF TABLES

Table 1: Summary of imaging modalities including their key characteristics, pros, and cons in the context of pTBI. 13
Table 2: Summary of studies measuring IHTT in pTBI cohorts 24
Table 3: Descriptions of the task MATLAB script parameters that contribute to the durations of the motor task features shown in the MATLAB script (figure 7) 31
Table 4: Summary of time parameters for the non-motor task 34
Table 5: Script descriptions for motor task output data 35
Table 6: Adult cohort profile including median age, sex, handedness, and report of a mood disorder. 40
Table 7: Demographic and injury details of pTBI cohort. 42
Table 8: The mean, minimum, first quartile, median, third quartile and maximum of the average number of incorrect trials for the motor tasks and total number trials removed during EEG pre-processing stages. 44
Table 9: Average IHTTs calculated from occipital and parietal sites in the adult cohort. 46
Table 10: Test-retest reliability scores for IHTTs calculated from the motor and non-motor tests for both parietal and occipital electrode sites. 48
Table 11: Inter-rater reliability scores for IHTTs calculated by the parietal and occipital sites 48
Table 12: Report on number of incorrect letter responses recorded for each session when pTBI participants completed the motor task. 49
Table 13: Calculated IHTTs for each visual field using waveforms from the O1-O2 electrodes sites for motor and non-motor tasks. 50

Chapter 1: Introduction

1.1 Overview

Traumatic brain injury (TBI) results from insult to the brain by an external mechanical force (Menon *et al.*, 2010; Thurman, 2016). The global incidence rate for paediatric TBI (pTBI) is disproportionately high and differs greatly by country, reporting to affect 43 - 280 per 100 000 children each year (Dewan *et al.*, 2016a). PTBI is currently one of the leading causes of mortality and morbidity in children and a major burden to public health systems globally. Children are at heightened risk for lifelong disability and early injury that may disrupt normal childhood development due to their underdeveloped brains (Catroppa *et al.*, 2008; Dismuke, Walker and Egede, 2015). Injuries sustained by pTBI are comparable to adults, however the literature shows that the pathophysiology and management differ. These differences can be attributed to the differences in mechanisms of injury as well as the age-related structural differences (Figaji, 2017). It is therefore necessary that more pTBI specific research is conducted for appropriate clinical management during the acute phase of injury, and further intervention to aid rehabilitation months and years following the initial injury.

While there are limited South African TBI epidemiology reports, it is believed pTBI incident rates are up to three-times higher in low-middle income countries (Nell and Brown, 1991; Dewan *et al.*, 2016a). Local TBI epidemiology studies report that pTBI rates in South Africa are particularly high due to the high motor vehicle accident (MVA) incidence rates, where pedestrian related MVAs account for the majority of pTBIs (Nell and Brown, 1991; Schrieff *et al.*, 2013). MVAs are the leading cause of morbidity and mortality in pTBI as it is associated with diffuse axonal injury that may lead to increased risk for adverse outcomes. The high incidence rate of TBI in the country further burdens the South African public health system in both primary care and rehabilitation facilities (Webster, Taylor and Balchin, 2015). The literature shows there are disparities in the treatment and rehabilitation of TBI depending on an individual's socioeconomic status (SES), where patients from lower SES are likely to have limited access to prognostic tools and rehabilitation programs (Haines *et al.*, 2019). In 2014 and 2015 the Living Conditions Survey showed that about half of the adult South African population lives under the upper-bound poverty line, which further compounds the economic burden associated with TBI, creating an inimical environment for favourable outcomes following injury (Statistics South Africa, 2015).

1.2 Clinical significance of the study

The primary goal of TBI clinical care is to manage the primary injuries from the initial insult and prevent the progression of secondary injury cascades that follow (Popernack, Gray and Reuter-Rice, 2015). The ability to assess the extent of brain injury as early as possible is important for appropriate prognosis of the injury (Suskauer and Huisman, 2009). The development of readily available and cost-effective tools for functional outcomes may allow one to identify individuals who are at risk for adverse outcomes following pTBI, and for appropriate allocation of resources to design individual-based rehabilitation plans to mitigate long term TBI sequelae. Once the child enters the sub-acute phase, early predictors may also assist in implementing early intervention that may improve neurocognitive and behavioural outcomes following injury.

Neuroimaging traditionally serves an important role in the acute setting to guide early medical or surgical intervention. Conventional neuroimaging modalities such as computed tomography (CT) scans are well established in the clinical setting to identify macroscopic injuries such as intracranial hematomas and brain contusion. However, they are limited in predicting long term outcomes due to their relative insensitivity to microscopic injuries such as diffuse axonal injury (DAI) (Lee and Newberg, 2005; Suskauer and Huisman, 2009). DAI is increasingly recognized as a cause of morbidity in TBI patients, and it is therefore important to detect the extent of DAI for appropriate long-term intervention.

In the past two decades magnetic resonance imaging (MRI) has become more widely available. Contrary to CT scans, MRI does not make use of radiation which allows for longer image acquisition times and provides high spatial resolution, with high signal and contrast to noise ratio (Doezema *et al.*, 1991). Further advancements in MRI technology such as diffusion weighted imaging (DWI) has allowed for the study of microstructural injuries in white matter (WM), and the use of diffusion tensor imaging (DTI) has demonstrated to be a promising imaging biomarker for DAI. Advanced MRI techniques are however still limited in providing structural outcomes (Suskauer and Huisman, 2009; Smith *et al.*, 2019). The literature shows that patients with similar imaging profiles will not necessarily have the same functional outcomes. There is still a need for robust and reliable predictor tools for functional outcomes of pTBI. Furthermore, advanced MRI techniques are not readily available in resource limited settings, are expensive to perform, time consuming and challenging to conduct in paediatric populations.

Interhemispheric transfer time (IHTT) has shown to be a promising tool in predicting functional outcomes post pTBI and serves as a tool to measure the functional integrity of the corpus callosum (CC). The corpus callosum is one of the most widely reported areas of damage in pTBI (Benavidez *et al.*, 1999; Wilde *et al.*, 2006; Wu *et al.*, 2011). Currently, there is no standardised method for measuring IHTT however methods using visual event-related potentials (ERPs) identified on electroencephalogram (EEG) recordings have demonstrated to provide more accurate estimates of IHTT due to the high temporal resolution that EEGs provide (Saron and Davidson, 1989; Brown *et al.*, 1999). Measuring IHTT could serve as a cheaper alternative to advanced MRI especially in resource limited settings, and appropriate for pTBI patients who suffered from diffuse injuries.

To date an ERP-based IHTT task has only been tested in one paediatric population (Dennis *et al.*, 2015, 2017; Ellis *et al.*, 2016). They found that pTBI patients with slow IHTTs had poor callosal WM microstructure and performed poorly on neurocognitive assessments (Dennis *et al.*, 2015; Ellis *et al.*, 2016). IHTT may therefore serve as a predictor of functional outcomes following pTBI. These studies however included older adolescent cohorts and made use of complex pattern matching tasks. These complex tasks may be too complex for a young pTBI cohort so there is a need to develop IHTT tasks that are not too cognitively loaded, and options available for patients who are unable to provide motor responses.

1.3 Research Statement

This study serves to present the development of two novel EEG-based IHTT tasks and investigate whether their application is appropriate for the local South African pTBI population. To date it also serves as the first time IHTT was investigated in a South African TBI cohort.

Chapter 2: Literature Review

2.1 Traumatic Brain Injury

2.1.1 Overview

Traumatic brain injury (TBI) is a broad term for a wide range of brain pathophysiology acquired by an external mechanical force to the head. The US Centers for Disease Control and Prevention describes that one or more of the following symptoms is attributable in TBI; (a) decreased or altered level of consciousness, or amnesia; (b) other neurologic or neuropsychological changes; (c) skull fracture; (d) traumatic intracranial lesions or (e) death (Thurman, 2016).

Clinical severity of TBI is usually measured by the Glasgow Coma Scale (GCS) and initially reflects the extent of injury to the brain by the primary event (Popernack, Gray and Reuter-Rice, 2015). The GCS is a 15-point scale comprising of three components: best eye response, best verbal response, and best motor response. It is scored from one for no response to normal values of four in eye-response, five in verbal response and six in motor response, resulting in a maximum score of 15 (Shobhit Jain and Iverson Affiliations, 2022). GCS scores of 13-15 are considered mild TBI, scores between nine and 12 are moderate TBI and scores of eight and below are considered severe TBI (Popernack, Gray and Reuter-Rice, 2015). While there appears to be some predictive value in the initial GCS score, where children with low initial GCS scores have increased risk for death or disability, TBI is incredibly heterogeneous where many factors influence functional outcomes (Lieh-Lai *et al.*, 1992; Cicero and Cross, 2013).

2.1.2 Primary mechanisms of Injury

The mechanisms of TBI can be classified as primary or secondary injury. Primary injuries result from the direct mechanical insult to the brain parenchyma and may result in focal or diffuse brain injuries however most injuries are heterogenous, consisting of both focal and diffuse components (Mckee and Daneshvar, 2015). Focal brain damage is caused by forces acting on the skull that results in compression of the tissue underneath, usually at the site of injury or directly opposite the site of impact (Pudenz and Shelden, 1946). These include contusions, intraparenchymal haemorrhage and subdural and epidural hematomas that tend to be localised and macroscopic in nature. Subdural haematomas can be extensive in younger children due to the lack of neuronal adhesions, and unlike adults are common in the interhemispheric fissure and along the tentorium (Poussaint and Moeller, 2002; Tang and Lim, 2009). Cortical contusions are less common in pTBI,

especially in younger children, because the inner table of their skulls are smoother compared to adults (Poussaint and Moeller, 2002). The young brain is also more likely to tear upon significant impact than contuse due to the soft consistency of the brain (Case, 2008).

2.1.3 Diffuse axonal injury

Diffuse axonal injury (DAI) is a process of widespread axonal damage due to sudden acceleration, deceleration, and rotational forces exerted to the brain concurrent or independent of direct impact (Meythaler *et al.*, 2001; Greve and Zink, 2009; Pinto *et al.*, 2012). These forces lead to shearing and tearing of axons that result in disruptions to neurofilaments of the axon cytoskeleton and disrupts normal axonal transportation mechanisms. This leads to the accumulation of axonal proteins in affected areas, forming retraction bulbs and triggers a set of secondary injury mechanisms (Angelova *et al.*, 2021). While the whole brain parenchyma undergoes tissues deformation during TBI, WM is at most risk due to the highly organized and anisotropic structure (Tang and Lim, 2009; Johnson, Stewart and Smith, 2013). The viscoelastic nature of axons helps axons return to their normal shape and structure during normal head movement, however when the threshold of maximum elasticity is exceeded it results in changes to the axonal integrity (Smith et al. 1999 Meythaler et al., 2001; Johnson, Stewart and Smith, 2013).

Following DAI, Wallerian degradation is widely observed (Meythaler et al., 2001). The compromised permeability of the axonal cellular membrane causes an increase in intracellular calcium concentration which triggers calpain mediated necrosis and mediates other self-destructive processes within the cell (Povlishock, 1991; Von Reyn *et al.*, 2012). In addition, the calcium overload also causes compromised permeability of the mitochondrial membrane leading to mitochondrial swelling. This leads to its inability to produce adenosine triphosphate (ATP) along with the production of oxidants leading to oxidative stress. Without the production of ATP the cell is unable to maintain the Na+ K+ and Ca2+ pumps, the cell is unable to maintain ionic homeostasis and the cycle of self-destruction continues. Metabolic failure and oxidative stress within the damaged axons activate inflammatory processes and recruitment of microglia as a response to mitigate the damage that has occurred. These processes tend to be progressive and delayed, similarly to other secondary injury mechanisms.

The corpus callosum, the brainstem and parasagittal WM and are commonly affected by DAI (Meythaler *et al.*, 2001; Pinto *et al.*, 2012). Children are particularly vulnerable to DAI due to the anatomical and biomechanical differences. Younger children’s heads are relatively larger

compared to older children and adolescents which are supported by weaker neck musculature and their underdeveloped WM may also contribute to decreased WM integrity following injury (Wu *et al.*, 2011; Figaji, 2017). It is also suggested that while there is a dose-dependent effect of DAI on neurocognitive impairment, the extent of secondary injury following the initial insult is a determining factor in progressive axonal deterioration and may contribute to WM atrophy in the affected areas (Lipton *et al.*, 2008).

Furthermore, while WM develops rapidly within the first 10 years of life, WM development is only complete in early adulthood (Muetzel *et al.*, 2008; Kochunov *et al.*, 2012). Compromised WM microstructure has been indicative of poor neurocognitive function (Benavidez et al., 1999; Dennis et al., 2015) further suggesting that pTBI patients are particularly vulnerable and DAI is increasingly recognized as an important cause in predicting functional outcome.

2.1.4 Secondary mechanisms of injury

Secondary insults occur once inflammatory and altered biochemical cascades are initiated by the onset of the primary insult. These injuries tend to be prolonged and progressive. Secondary insults include altered cell metabolism, oxidative stress, inflammation, and cerebral oedema.

Neuroexcitoxicity and altered cell metabolism.

Massive and widespread depolarisation of neurons, glial cells and endothelial cells are one of the initial secondary injury responses to TBI (Kaur and Sharma, 2018). Excessive glutamate is thought to be involved in this process and is also a significant contributor to cell death where alterations in presynaptic and postsynaptic glutamate receptors contribute to excitotoxicity (Bullock *et al.*, 1998; Kaur and Sharma, 2018). Microdialysis studies show that excessive extracellular glutamate is associated with adverse outcomes (Bullock *et al.*, 1998; Koura *et al.*, 1998). The excessive release of glutamate also mediates the disruption of calcium homeostasis (Choi, 1987). The influx of calcium leads to disruption of microtubule construction, protease formation and other enzyme function within the cell (Pike *et al.*, 2000). Excessive calcium can also lead to mitochondrial swelling and eventually loses its ability to produce adenosine triphosphate (ATP) (Lifshitz *et al.*, 2003; Singh *et al.*, 2006). The reduction in ATP production prohibits the cell from maintaining cellular functions and maintaining ionic homeostasis (Marklund *et al.*, 2006). In addition, the loss of mitochondrial function may initiate cell death via apoptosis or indirectly though the loss of oxidative phosphorylation (Bü ki *et al.*, 2000; Robertson, Saraswati

and Fiskum, 2007). To minimise the extent of secondary insults is the primary goal in the management of TBI patients.

Sources of brain oedema and raised ICP.

Severe cases of TBI often causes breakdown of the blood brain barrier (BBB). The leaky BBB results in vasogenic fluid to accumulate in the brain that causes brain oedema. Cytotoxic brain oedema also occurs due to the neuroexcitoxicity that is initiated by the excessive release of glutamate and the cells' failure to maintain ionic homeostasis (Unterberg *et al.*, 2004). Cytotoxic brain oedema involves intracellular water accumulation that occurs independently of BBB breakdown (Unterberg *et al.*, 2004). These sources of oedema in combination with brain haemorrhage and haematomas contributes to raised ICP and decreased cerebral perfusion. The brain is housed within the rigid skull cavity with limited ability to compensate for increased brain volume and pressure (Michinaga and Koyama, 2015). Persistent elevated ICP and reduction in brain oxygenation heighten the risk for ischaemia or brain herniation and is associated with increased risk for poor outcomes (Kaur and Sharma, 2018). Hours following TBI vasogenic fluid accumulating in the brain causes cerebral oedema that contributes to raised ICP and decreased cerebral perfusion (Ghajar, 2000; Greve and Zink, 2009). The brain in housed within the rigid skull cavity with limited ability to compensate for brain oedema and haematomas(Mohseni-Bod, Drake and Kukreti, 2014). Persistent elevated ICP and reduction in brain oxygenation heightens the risk for ischaemia or brain herniation and is associated with increased risk for poor outcomes (Case, 2008).

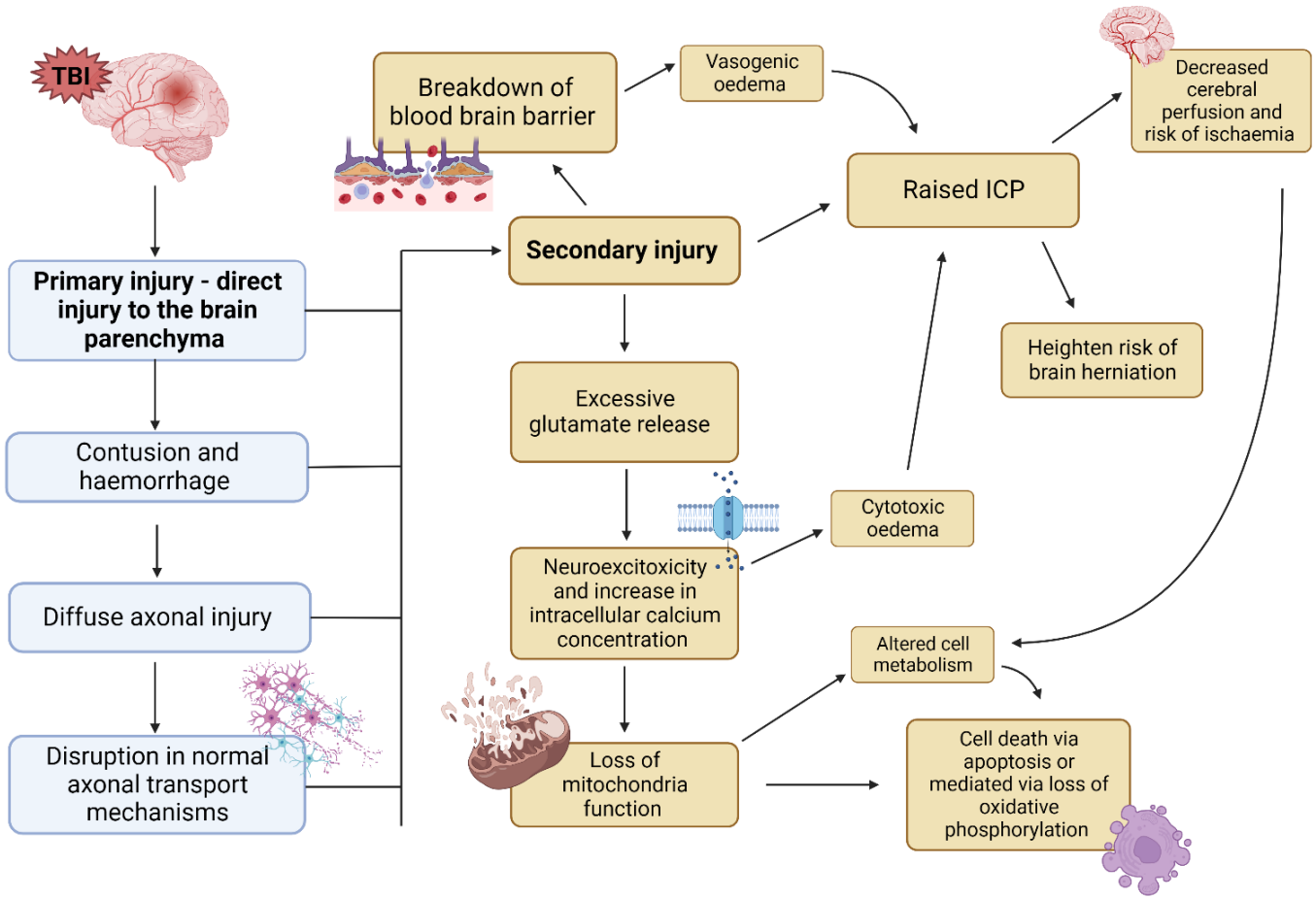

Figure 1: Pathophysiology of TBI; the diagram above aims to depict the pathophysiology of TBI from the moment of impact. The primary insults are depicted in blue including contusion, brain haemorrhage and diffuse axonal injury. These injuries result from the direct injury to the brain parenchyma and almost instantaneously. All these contribute to the secondary insults that are depicted in orange. The diagram shows that ICP arise from multiple origins including the breakdown of the BBB, brain swelling and bleeding, where prolonged raised ICP is generally associated with poorer outcomes because patients are at higher risk for ischaemia and brain herniation. While it may appear that these mechanisms occur in linear manner, usually they tend to occur simultaneously and may continue hours and days following the initial injury (diagram created with Biorender).

2.2 Outcome and predictors of functional recovery following paediatric traumatic brain injury.

2.2.1 Outcomes of traumatic brain injury

Outcomes following pTBI tend to be heterogenous, further complicating prognosis for individual cases however, there seems to be a dose-dependent relationship between severity and injury outcome. The literature consistently reports that moderate-severe pTBI patients tend to perform poorer than mild pTBI and control participants on neurocognitive assessments in the sub-acute phase of injury in measures of intelligence, attention, processing speed, visual spatial processing and working memory (Van Heugten *et al.*, 2006; Babikian and Asarnow, 2009). Moderate-TBI patients tend to perform similarly to control patients in memory and visual perceptual skills once recovery is complete, usually about 2 years following injury. Longitudinal studies following severe pTBI patients for 2 or more years show that there are persistent neurocognitive impairments in a cluster of children with severe TBI (Babikian and Asarnow, 2009; Allen *et al.*, 2010). Even though some recovery has taken place they continue to not only fail to catch up to their control counterparts but appear to fall farther behind over time (Jonsson *et al.*, 2013). These persistent neurocognitive impairments ultimately lead to more negative consequences such as a lack of independence and increases the family burden of injury (Catroppa *et al.*, 2008).

2.2.2 Predictors of Outcome

There are various factors that influence outcomes following TBI. Studies consistently report that children with severe injury in early childhood – infants who are a few months old up until six-year-olds – are at increased risk for adverse outcomes following injury and rehabilitation (Prasad *et al.*, 2002; Catroppa *et al.*, 2008; Prigatano and Gray, 2008; Jonsson *et al.*, 2013). Recovery curves in older children and adolescents show significant improvements in neurocognitive measures and IQ scores 3-6 months post injury, followed by minimal change two years after injury. In younger children, however, these curves appear to be flatter with minimal changes in neurocognitive measures and IQ scores over time following TBI (Prigatano and Gray, 2008). There are several mechanisms that hypothesize why this may be the case. Structurally younger children's relatively large heads are supported by weak neck muscles, making them for more vulnerable for DAI to the immature brain (Mendelsohn *et al.*, 1992; Poussaint and Moeller, 2002; Case, 2008; Figaji, 2017). The damaged neural systems of the immature brain that are responsible for skill acquisition may also accounts for greater disruption in cognitive development (Taylor and Alden, 1997).

Adverse outcomes following TBI are further compounded when children come from low social economic backgrounds. Patients who do not have medical aid or insurance tend to be more vulnerable and contribute to the disparity in treatment and functional outcomes. These patients are more likely to be discharges early and have limited access to rehabilitation to aid recovery (Haines *et al.*, 2019).

2.3 The use of neuroimaging in TBI

2.3.1 Neuroimaging in the acute phase of TBI

Computed tomography

Computed tomography (CT) is an imaging modality that uses narrow X-ray beams that rotates rapidly around a patient. As the x-rays leave the body, they are picked up by x-ray detectors, which then sends signals to a computer to produce cross-sectional slices of the area of interest (Hathcock and Stickle, 1993). The use of CT is firmly established in the acute setting of TBI because it renders images in a short acquisition time, it is readily available and easy to use in patients who are ventilated (Poussaint and Moeller, 2002). CT scans are sensitive in detecting conditions that require emergent intervention such as hematomas with brain herniation and midline shift (Kelly *et al.*, 1988; Poussaint and Moeller, 2002). The use of fast multidetector CT has contributed to dramatically reduced scanning times and allows for quick rescanning of slices affected by motion artifact (Jones *et al.*, 2001).

Magnetic resonance imaging (MRI) is a non-invasive imaging technique that takes advantage of strong body's magnetic properties with the use of the hydrogen nucleus due to its abundance in water and fat (Berger, 2002). Standard MRI has become more readily available in acute TBI settings and offers high spatial resolution, high contrast, and high signal to noise ratio (Suskauer and Huisman, 2009). MRI does not make use of ionising radiation like CT scanning and allows for longer image acquisition times that offers increased diagnostic accuracy. MRI have greater sensitivity in detecting DAI, haemorrhagic punctate lesions, and subtle neuronal damage. Is better at detecting small areas of contusion, DAI, and subtle neuronal damage (Levin *et al.*, 1987; Ogawa *et al.*, 1992).. Studies have shown that MRI detects 10-20% of abnormalities missed by CT, (Doezema *et al.*, 1991; Mittl *et al.*, 1994).

Detecting the full extent of DAI is usually challenging, especially in the acute setting. The same forces that cause the shearing and tearing of axons are also believed to stretch and rupture small blood vessels that run in parallel with axons, causing punctate haemorrhages (Tang and Lim, 2009). These punctate haemorrhages can be viewed on a CT and standard MRI scan however, less than 40% of DAI lesions are haemorrhagic (Meythaler *et al.*, 2001; Blackman *et al.*, 2003). While CT and standard MRI are ideal for detecting focal injuries, they are not sensitive enough to detect the full extent of DAI due to the widespread and microscopic in nature of DAI.

2.3.2 Diffuse Tensor Imaging

Diffuse weighted imaging is an advanced MRI modality that generates signal contract based on differences in water Brownian diffusion (Baliyan *et al.*, 2016). The brain is mode of 73% water and in free space water diffused freely in an isotropic manner (Baliyan *et al.*, 2016). Water diffusion in WM tends to be anisotropic due to the highly organized nature of WM bundles (Razenberger LR, 2022). DTI exploits this can provide sensitive measures on the microstructural integrity of WM. DTI has therefore demonstrated to be more sensitive in detecting the extent of WM damage compared to standard MRI and CT (O'Donnell and Westin, 2011). Fractional anisotropy (FA) is a measure provided by DTI analysis to assess the directionality of water diffusion and is measured between 0 and 1, where low FA indicates that diffusion is isotropic and higher FA values suggest anisotropic diffusion. Low FA values are indicative of damage to the fibre tracts as the diffusion of water is not restricted to just one axis (Kochunov *et al.*, 2012; Strangman *et al.*, 2012). DTI tractography also allows one to skeletonize and reconstruct WM tracts of the brain in 3D to visualise damaged WM areas in the brain in more detail (Wakana *et al.*, 2004; Johansen-Berg and Behrens, 2006).

DTI has increasingly been used as an imaging biomarker for predicting functional outcomes (Hulkower *et al.*, 2013; Song *et al.*, 2015). In pTBI studies, the literature shows that low FA values are associated with lower performance on neurocognitive tests, hinting at associations between compromised WM development and poor neurocognitive functioning and development in children (Strangman *et al.*, 2012; Dennis *et al.*, 2015; Ewing-Cobbs *et al.*, 2016).

Limitations of DTI

While FA values are sensitive, they are not specific to TBI and for accurate interpretation and increased specificity findings need to be combined with clinical history and the findings of conventional imaging (Razenberger LR, 2022). Normal paediatric FA values are also lower than adults and it is only by age 11 that 90% of normal adult FA values are achieved (Feldman *et al.*, 2010). Currently DTI also has a low signal to noise ratio (SNR) and requires longer scanning times. One can shorten the image acquisition time by reducing the SNR, but this will provide poor image quality (Farrell *et al.*, 2007). Longer image acquisition times also provide the risk of patient motion that can cause artefact. Lastly, even though DTI offers great spatial resolution it is still unable to elucidate the underlying mechanisms at the microscopic level that are responsible for the disruptions in WM structure.

2.3.3 Magnetic resonance spectrometry

Magnetic resonance spectrometry (MRS) was developed to complement advanced MRI techniques such as DTI. MRS is a modality that provides insight on biochemical changes that may exist due to injury to the brain, such as TBI. It provides information on levels of neurometabolites such as N-acetyl aspartate (NAA) and choline (Cho). NAA is a marker used for neural and axonal integrity whereas Cho is a marker of inflammation and membrane integrity (Ashwal *et al.*, 2000, 2006). The research shows that moderate-severe pTBI patients present with lower levels of NAA and higher levels Cho post TBI when compared with control participants and predictive value for degree of WM atrophy and integrity (Ashwal *et al.*, 2000; Sinson *et al.*, 2001). A recent pTBI MRS study shows that patients who had higher information processing speed had higher NAA and minimal WM disruptions, whereas those with slow information speed had low NAA levels and also presented with lower FA in DTI analysis in the relevant WM tracts (Dennis *et al.*, 2018). MRS in conjunction with DTI may also serve as a predictor of functional outcomes.

Table 1: Summary of imaging modalities including their key characteristics, pros, and cons in the context of pTBI.

Imaging Modalities	**Key Characteristics**	**Pros**	**Cons**
Computed tomography (CT)	Computerized procedure that produces cross sectional images/tomographic slices with the use of X-ray beams that rotate around the patient.	Widely available Renders images quickly Ideal for identifying conditions that require emergent intervention	X-rays produce ionizing radiation and do not allow for long image acquisition times. Children are more sensitive to ionizing radiation and at a higher risk associated with exposure to radiation. Tends to underestimate the extent of punctate contusions.
Magnetic resonance Imaging (MRI)	Takes advantage of the body's own magnetic properties to produce	Does not make use of ionizing radiation, therefore non-	Cumbersome to perform in ventilated patients.

	images with high contrast.	invasive and safe for the paediatric brain. Offers high spatial resolution, contrast, and signal to noise ratio. More sensitive to small areas of contusion and neuronal damage.	Are not widely available. Challenging to carry out in children because the MRI is very sensitive to motion that can create artefacts. Cannot be used on patients with any kind of metal implant.
Diffuse weighted imaging (DWI) and diffuse tensor imaging (DTI)	Generates signal contrast based on the differences in Brownian diffusion. Water diffusion in WM is anisotropic due to its highly organized nature. DTI can therefore assess the microstructural integrity WM following injury.	FA is very sensitive to WM microstructural change Research shows DTI may serve as a biomarker for functional outcomes of TBI	Currently offers low signal to noise ratio and has a long image acquisition time. Not widely incorporated into routine clinical practice. While FA measures are highly sensitive there are not specific.
Magnetic resonance spectroscopy (MRS)	Provides insight on levels metabolite levels in the brain such as NAA and Cho. NAA often used as a biomarker for neural and axonal integrity in the brain. Cho is a biomarker for inflammation and membrane integrity.	Non-invasive method to investigate biochemical changes following injury.	No standard clinical protocol available. Not widely available

2.3.4 Limitations of advanced neuroimaging

While advanced MRI modalities have shown to provide prognostic value and provide great spatial resolution, obtaining these images in the acute stage of injury is still impractical as they are time consuming and very expensive to perform. Even in the recovery phase it is a challenge to perform these scans on younger children as they are required to lie still for extended periods for optimal resolution. While DTI is more sensitive to WM changes and a promising biomarker, it is still limited to only providing information on structural integrity and morphological changes of the affected brain areas. There remains limited insight on the underlying pathophysiological changes and ability to identify patients particularly at risk for adverse functional outcomes months following the initial injury.

2.4 The corpus callosum

2.4.1 Corpus callosum anatomy and function

The corpus callosum (CC) (figure 2) is the main commissural region of the brain, located along the midline and houses the largest WM bundle in the brain (Kathleen Baynes, Encyclopaedia of the Human brain, 2002. The CC contains approximately 200 million fibres and connects the two cerebral hemispheres where its primary function is to transfer and integrate information between the two hemispheres (Tanaka-Arakawa *et al.*, 2015). The CC is organised topographically where the anterior portions are involved in the transfer of high cognitive function and the posterior portions including the posterior midbody, isthmus and splenium are involved in the transfer of auditory, somatosensory and visual information, respectively (Fabri *et al.*, 2014; Tzourio-Mazoyer, 2016).

Communication between the two hemispheres is imperative for proper processing of sensory information and higher order cognitive function (Fabri *et al.*, 2014). While the CC is developed by early childhood, myelinization is believed to only be complete by the onset of puberty and it continues to grow and mature well into the third decade of life (Giedd *et al.*, 1996; Muetzel *et al.*, 2008; Kochunov *et al.*, 2012). WM development of the CC into adulthood facilitates motor skill refinement and improved cognitive development ((Muetzel *et al.*, 2008; Chevalier *et al.*, 2015).

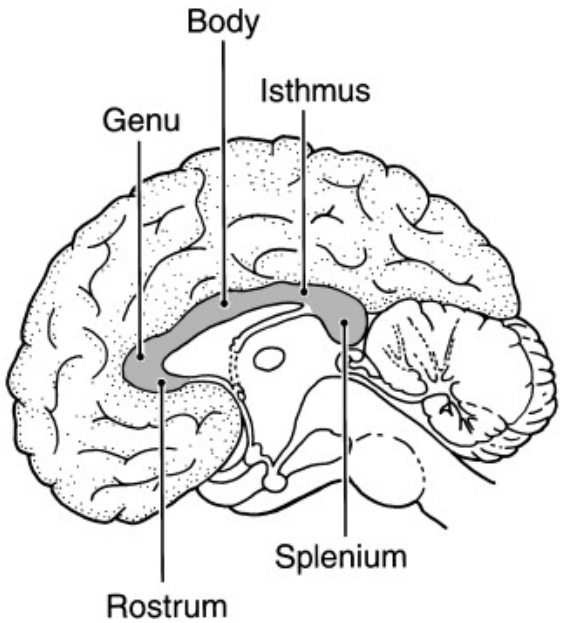

Figure 2: Sagittal section of the brain that slices through the midline locating the major regions of the CC. The rostrum is the most anterior portions of the CC that connects the orbital surfaces of the frontal lobes. The genu connects the medial and lateral surfaces of the frontal lobes. Posterior portions including the posterior midbody, isthmus and splenium are involved in transfer of somatosensory information and connects to the parietal, temporal and occipital lobes.

2.4.2 Damage to the corpus callosum following TBI

The CC is one of the most widely reported regions of disruption following TBI and is particularly vulnerable to DAI and progressive axonal disruption (Hulkower et al., 2013). The most posterior portion of the CC, the splenium, has shown to be the most vulnerable to damage. It is suggested that upon impact during injury the falx cerebri prevents the splenium from moving further amplifying the acceleration and deceleration forces on the splenium (Benavidez *et al.*, 1999). Imaging studies show there is significant atrophy and compromised WM microstructure in all regions of the corpus callosum in a cluster of moderate-severe pTBI patients months following TBI (Wu *et al.*, 2011; Dennis *et al.*, 2015, 2017). On the contrary control groups show increased callosal volumes that is consistent with developmental changes in the age group (Wu *et al.*, 2011).

2.5 Interhemispheric Transfer time

2.5.1 Neural wiring of the visual system

The neuroanatomy of the visual system (figure 3, image by Miquel Perelló Nieto) has allowed for one to investigate interhemispheric interaction. When visual information falls on the retina, information in the right visual field (RVF) falls on the left side of both eyes and information in the left visual field (LVF) falls on the right half of the retina of both eyes. Both eyes receive similar information about the world, except for the far portion of the periphery. The optic nerve from each eye carries the visual information exclusively from that eye and meet at the optic chiasm where information from the nasal hemiretina cross over to the opposite side of the brain – axons from neurons that carry information from the RVF come together, and those from the LVF come together (Banich, 2003).

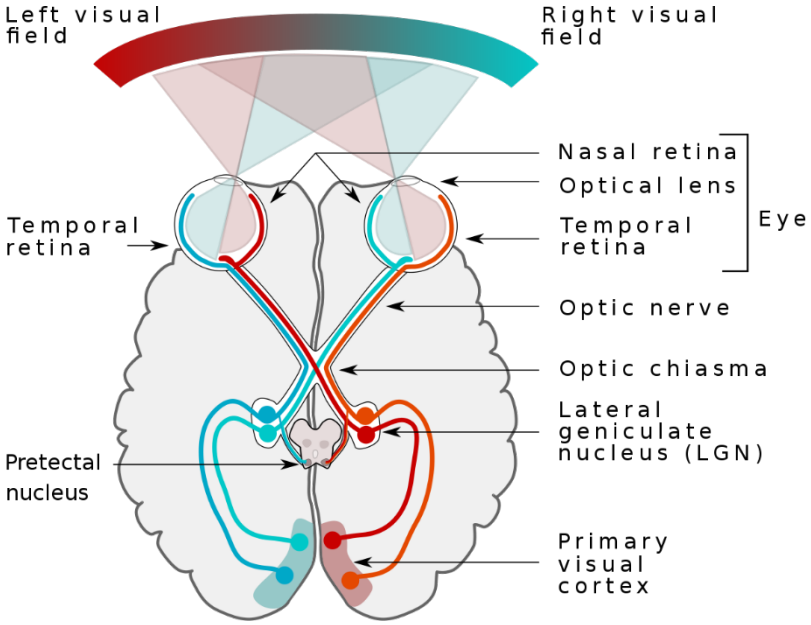

Figure 3: Schematic of the visual pathway from the eyes to the brain. Depiction of how all visual information from the RVF is first processed by the left hemisphere and vice versa for the information from LVF.

Beyond the optic chiasm, once the axons have been reorganised, the optic tract for each visual field then synapses on the lateral geniculate nucleus of the thalamus and course upwards to the primary visual cortex. When information first reaches the primary visual cortex, it exclusively represents information from the contralateral visual field. Information from the LVF will be mapped in the right hemisphere, and information from the RVF will be mapped in the left hemisphere.

Visual information is then shared with the ipsilateral hemisphere via the corpus callosum for higher order integration (Banich, 2003).

Given that the corpus callosum is responsible for interhemispheric communication between the two cerebral hemispheres, researchers have suggested interhemispheric transfer time (IHTT) may be used to assess the functional integrity of the corpus callosum (Brown *et al.*, 1999; Peru *et al.*, 2003). IHTT measures transfer time of information from one hemisphere, across the corpus callosum to the other hemisphere. An early task reaction study established slower IHTTs in children following TBI, which is associated with slower information transfer between the hemispheres (Benavidez *et al.*, 1999). Imaging studies have also shown that there are significant differences in the WM integrity in pTBI patients with slower IHTTs and perform significantly poorer on neurocognitive assessments (Dennis *et al.*, 2015, 2017). This suggests that IHTT could serve as a predictor of neurocognitive outcomes following pTBI.

2.5.2 Early studies of interhemispheric transfer time

The Poffenberger paradigm

In the early 1910s A.T Poffenberger conducted a few visual reaction time experiments while investigating new synaptic theories. He was the first to demonstrate that interhemispheric transfer time could be measured with a visuomotor reaction time task. As explained before, he reasoned that anatomically each visual field first projects to the visual cortex in the contralateral occipital lobe and then transfers the visual information to the ipsilateral hemisphere. If a participant reacts to a visual stimulus by pressing a key with a hand on the same side, direct intra-hemispheric connections between the visual and motor cortex will result in a fast response. However, when the participant reacts with the opposite hand, interhemispheric transfer of the visual cortex to the motor cortex of the ipsilateral hemisphere is required for a response and yields a longer reaction time. He hypothesised interhemispheric transfer time could be measured by subtracting the mean crossed visual field hand conditions from the mean uncrossed visual field conditions and observed that crossed responses took longer than uncrossed response (Braun, Collin and Mailloux, 1997; Marzi, 1999).

Simple Reaction Estimates of IHTT

Early reaction time tasks consisted of a simple motor response to an unpatterned stimuli briefly presented in the LVF or RVF. Each trial would randomly present a fixation stimulus, with a duration of 1-3 seconds to prepare participants for the response. The fixation stimulus ensured against lateral shifts in gaze and controlled for the presentation of the visual stimuli in the appropriate

visual field. Following the fixation point the lateral visual stimuli would present to the RVF or LVF and the participant would respond with a unimanual or bimanual response for every single trial in the task (Marzi, 1999).

For decades simple reaction time tasks were considered to provide the most reliable estimates of IHTT, however differences in unimanual and bimanual responses to these tasks were reported. In addition, there appears to be an inverse relationship in reaction time and IHTT in unimanual versus bimanual responses. Unimanual responses have short reaction times, but longer estimates of IHTT, whereas bimanual responses provide longer reaction times and shorter IHTT and the cerebral mechanisms responsible for the differences were still poorly understood and has yet to be experimentally separated. Unimanual responses however have demonstrated to provide more consistent estimates of IHTT from reaction time tasks (Bashore, 1981). It was thought that longer reaction times observed in bimanual responses may result from central interference phenomena that accounts for interlimb competition in more complex motor task and the reduction in IHTT may reflect premovement priming. It was therefore deemed inappropriate to treat IHTT measures from unimanual and bimanual responses as equivalent.

Stimulus-response compatibility effects may interact with intra and interhemispheric information processing to alter both reaction time and IHTT (Anzola *et al.*, 1977). The hemispheres differ in their ability to process simple visual input and execute uncomplicated motor responses (Bashore, 1981). There is also evidence of asymmetry in stimulus processing, where in right handers the right hemisphere is particularly fast in processing simple visual stimuli and the left hemisphere can execute motor responses more rapidly (Jeeves and Dixon, 1970; Anzola *et al.*, 1977).

Two-choice reaction tasks are when the participant is presented with two stimuli, each that requires a different response. These tasks also make use of unpatterned visual stimuli and simple motor responses. Two-choice reaction tasks investigations have shown that they are particularly sensitive to spatial relations, because motor responses will depend on where the stimulus is presented (Bradshaw and Perriment, 1970; Harvey, 1978). Estimates of IHTT from two-choice reaction tasks tend to be longer when compared with simple reaction tasks and stimulus detection and are more commonly used in investigations regarding spatial compatibility (Bradshaw and Perriment, 1970).

The literature shows that reaction time-based methods for measuring IHTT are too variable to provide reliable estimates of IHTT, suggesting behavioural reaction tasks are insensitive to measuring IHTT and may undermine complex visuomotor connections and other mechanisms involved in intra and interhemispheric transfer (Westerhausen *et al.*, 2006; Friedrich *et al.*, 2017). The best characterization of IHTT could be achieved by electrophysiological methods (Ledlow, Swanson and Kinsbourne, 1978; Brown and Jeeves, 1993).

2.5.3 Electrophysiological measures of IHTT

An electroencephalogram (EEG) is a non-invasive electrophysiological technique that records electrical activity from the brain. Hans Berger reported that human brain activity could be measured by placing electrodes on the scalp, amplifying the signal and plotting changes in voltage over time (Berger 1929). An EEG therefore reflects electrical activity of large populations of neurons synchronously firing and offers high temporal resolution that allows for the evaluation of dynamic cerebral activity (St. Louis *et al.*, 2016). Usually, EEG data cannot be used in its raw form to investigate specific neural processes, because the EEG represents an amalgamation of different neural sources of activity. Within the EEG are neural responses associated with specific sensory, cognitive, and motor events that can be extracted by an averaging technique (Luck, 2014). These specific responses are called event related potentials (ERPs) and indicate that they are electrical potentials related to specific events (Woodman, 2010). Averaging techniques allows one to isolate these ERPs by effectively cancelling random noise picked up on the EEG (Davis *et al.*, 1939; Woodman, 2010). Even with the invention of functional MRI techniques, ERP research continues to thrive due to the high-resolution temporal information that cannot be obtained any other way.

ERPs have demonstrated to serve as a more direct and reliable measure of IHTT due to the high temporal resolution provided an electroencephalogram (EEG) recording compared to the simple reaction time tasks (Ledlow, Swanson and Kinsbourne, 1978; Brown and Jeeves~, 1993; Woodman, 2010). A visual ERP waveform consists of peaks and troughs (figure 4; image by Chaumillon, Blouin and Guillaume, 2018) also known as ERP components, that are consistent and allows one to study information processing and other higher order cognitive processes. The EEG components, from both hemispheres, particularly at the parietal and occipital sites, can provide contralateral and ipsilateral conditions of the visual stimuli (Brown et al., 1994 and Woodman, 2010). When the waveforms of these EEG recordings are averaged it cancels out the random noise and allows one to visualize the visual ERP components more clearly, where early

waves of a visual ERP contain the large negative N1 and large positive P1 component. Early studies of ERP IHTT studies in healthy participants consistently show that there is a latency between the N1 peaks when the waveforms of the contralateral and ipsilateral conditions are overlapped (Brown and Jeeves, 1993; Brown *et al.*, 1999). Brown and Jeeves found that the N1 peak of the visual ERP provided an unconfounded measure of IHTT and studies following continue to use the N1 components to calculate IHTT (Brown and Jeeves, 1993). It has been suggested that the latency between the ipsilateral N1 peak and contralateral N1 represents the IHTT.

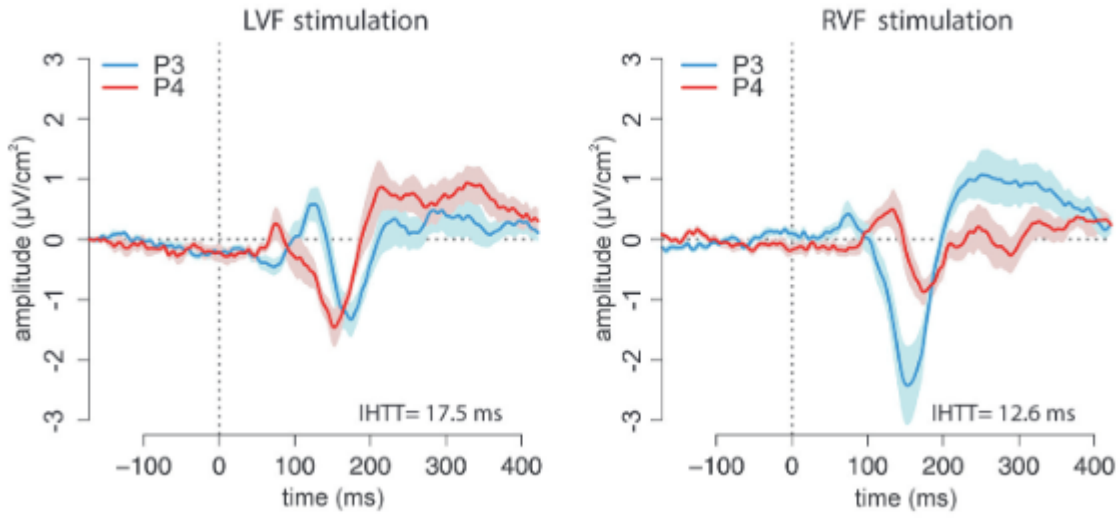

Figure 4: Overlapped averaged waveforms from parietal sites P3 and P4 displaying ERPs produced after visual stimulus onset. For RVF stimulation P3 electrode is the placed on the contralateral hemisphere and the P4 electrode is placed above the ipsilateral hemisphere. The most negative peak (N1) of the contralateral hemisphere appears before that of the ipsilateral hemisphere. The latency between the respective N1 peaks represents the IHTT (Chaumillion et al 2018).

2.5.4 IHTT measures in pTBI cohorts

Dennis et al. (2015, 2017) and Ellis et al. (2016) at the University of California, Los Angeles (UCLA) were the first to measure IHTT in a pTBI cohort using electrophysiological methods. They were able to identify patients with slow and normal IHTT within their pTBI cohort, when compared to their controls and showed that those with slow IHTT scored significantly lower on neurocognitive tests (Dennis *et al.*, 2015; Ellis *et al.*, 2016). The same group also demonstrated that there were significant differences in FA across four CC tracts between the normal-IHTT TBI group and controls (Dennis *et al.*, 2015). This suggests that structural biomarkers are not always indicative of functional outcome and perhaps a multimodal approach is necessary for accurate diagnosis and prognosis.

Dennis et al. (2017) showed that pTBI patients with slow IHTT showed significant decrease in volume in WM clusters, while some pTBI patients who had IHTTs within the normal range showed both increased and decreased volume in certain areas. This demonstrates that while some patients who experience moderate-severe pTBI demonstrate callosal atrophy, others show signs of recovery and normal brain development. They were also unable to show any significance between FA and IHTT and further highlights that while the structural integrity of WM provides some insight, one cannot solely rely on structural analysis for the prediction of functional outcome. This team made use of a pattern matching task that required motor responses (Ellis et al., 2016). However, after TBI children may have motor difficulties and may be physically unable to carry-out these motor responses for the IHTT tasks ((Gagnon, 1998). Additionally, their executive function may be affected and present with slower processing speed post injury, which may contribute to difficulty in completing a complex task (Babikian and Asarnow, 2009; Babikian *et al.*, 2011).

Table 2: Summary of studies measuring IHTT in pTBI cohorts.

Study Author	Study Aim	Cohort size, age and TBI severity	IHTT measuring technique(s)	Study findings
Benavidez et al (1998)	To evaluate the relationship between CC atrophy to IHTT following closed head injury.	51 pTBI patients split into three subgroups. *Mean age measured at testing Mild TBI: n = 14; mean age = 11.53 (1.81) years Extracallosal lesions: n = 20; mean age = 12.30 (2.31) years CC lesions: n = 17; mean age = 12.30 (2.46) years 16 control children; mean age = 12.17 (2.22)	Measured degree of asymmetry in performance on various tasks including: Verbal and non-verbal dichotic listening Motor and tactile tests Verbal and non-verbal tachistoscopic tasks	Severe pTBI patients with CC atrophy and lesions were associated with increased right ear advantage on verbal dichotic listening tasks. No significant differences between groups in asymmetries measured by the motor and tactile tests.
Dennis et al. (2015)	To examine the outcome heterogeneity within pTBI patients by assessing callosal function and callosal structural integrity.	35 moderate-severe pTBI patients. Cohort split into normal vs slow IHTT groups. pTBI normal: n = 16; mean age 14.5 (3.2) years	Visual ERPs – EEG recorded while participants completed a pattern matched task 3-5 months post injury. Callosal integrity examined by performing	TBI group was split into the two “slow” and “normal” subgroups based on the heterogeneity in IHTT measures within the group.

		pTBI slow: n = 16; mean 13.9 (2.5) years 31 control children; mean age 14.9 (3.0) years	tractography on DWI scans and measuring FA and mean diffusivity of selected WM tracts.	FA was significantly higher in 17 tracts in controlled group compared to pTBI-slow subgroup. FA was significantly higher in 4 tracts in the control group when compared to pTBI-normal sub-group. Also found that higher FA in CC frontal tracts were positively associated with better cognitive performance
Ellis et al. (2016)	To investigate correlations between IHTT and performance on neurocognitive tests in moderate-severe pTBI patients	44 moderate-severe pTBI patients. Cohort split into normal vs slow IHTT subgroups (as explain in Dennis et al 2015). pTBI normal: n = 26; mean age 14.6 (3.3) years pTBI slow: n = 18; mean age 14.3 (2.4) years	Visual ERPs – EEG recorded while participants completed a pattern matched task.	The slow-IHTT subgroup had significantly slower IHTT times than control group and performed significantly poorer on the neurocognitive assessments. There were not significant differences in IHTT and cognitive composite index between the pTBI

		39 control children; mean age 15 (3) years		normal and control groups. No significant differences in IQ between all three groups.
Dennis et al. (2017)	To assess longitudinal changes in regional brain volumes in a pTBI cohort compared with IHTT measured during subacute phase of injury.	21 moderate-severe pTBI patients. Cohort split into normal vs slow IHTT subgroups (as explain in Dennis et al 2015). Age at session 1: pTBI normal: n = 10; mean age 16.0 (2.6) years pTBI slow: n = 11; mean age 14.1 (1.9) years 26 control children; mean age at test 1 = 14.5 (3.0) years	Visual ERPs – EEG recorded while participants completed a pattern matched task. MRI scans also acquired at 2-5 months and 13-19 months post injury. Assessed longitudinal brain volume changes using tensor-based morphometry on T1-weighted images.	The TBI-slow group had significant atrophy in the CC, hypothalamus, and other grey and WM clusters. TBI patients with normal IHTT showed volume increases in the bilateral internal capsule, overlapping with the thalamus. Also found significant associations between regional brain volumetric changes and neurocognitive performance.
Olsen et al. (2020)	To investigate how working memory load dependent blood oxygen level dependent (BOLD) activation was related to measures of	18 moderate-severe pTBI patients. Cohort split into normal vs slow IHTT subgroups (as explain in Dennis et al 2015).	Visual ERPs – EEG recorded while participants completed a pattern matched task.	Study found that BOLD hyperactivation in moderate-severe pTBI patients are associated with IHTT. The TBI-slow group had greater

	IHTT in a moderate-severe pTBI cohort.	pTBI normal: n = 11; mean age 14.33 (2.67) years pTBI slow: n = 7; mean age 15.28 (2.09) years 26 control children; mean age 15.78 (3.12) years	T2-weighted BOLD fMRI acquired while patients performed a spatial working memory task.	BOLD activation and higher working memory load compared to control and TBI-normal groups. This was observed in widespread brain areas including the frontal, parietal and occipital regions. Associations between hyperactivations and age, time post-injury or neurocognitive performance index in T BI group were not significant.

2.6: Aims and Objectives

2.6.1 Aim

The aim of this study was to explore the development of two ERP-based IHTT tasks and to assess their potential application within a pilot group of children who had previously sustained a moderate to severe TBI.

2.6.2 Objectives

1. To describe how and why the IHTTs were developed.

Previous pTBI studies that measured IHTT with electrophysiological methods made use of complex tasks that may not be appropriate for a young pTBI cohort. For this study two tasks were developed; (1) a motor task that should be simple and not too cognitively loaded for young participants to carry out and (2) a non-motor task that may also serve as an alternative for participants who are unable to appropriate provide motor responses.

2. To provide feasibility reports and assess the reliability of the tasks with the use of an adult cohort.

Before conducting the tasks within a young pTBI cohort we had to ensure that (1) adults were able to comfortably complete the tasks, (2) the tasks produce reliable ERPs on an EEG and (3) the tasks provided moderate to high test-retest and interrater reliability.

3. To assess the feasibility of the tasks within a young pilot moderate severe pTBI cohort.

Once the tasks were validated, a pilot pTBI cohort was recruited to assess if the tasks were appropriate for a young pTBI cohort and enabled measurement of IHTT.

Chapter 3: Methodology

3.1 Development of the IHTT Tasks

3.1.1 Overview

Two IHTT tasks were developed for this study. The tasks are based on the divided visual field technique, which requires participants to focus on a fixation point while visual stimuli are briefly presented to the RVF or LVF (Banich, 2003; Bourne, 2006). The scripts for the tasks were developed on MATLAB R2016a (Mathworks, Natick, MA) and the Psychtoolbox-3 software package was used to display the tasks and visual stimuli in the form of a checkerboard pattern to produce a visual ERP. They were presented on a Dell Vostro 5590 10th Gen laptop with a screen size of 39.6cm and display resolution of 1920 x 1080 pixels. The first task involved motor responses, based on a MATLAB script provided by Tiffany Ho, with further work by Rupa Mahahedvan. It was developed further in collaboration with Emily Dennis, Robert Asarnow and Warren Brown from UCLA. The second task involved no motor responses but presented the visual stimuli in a similar manner.

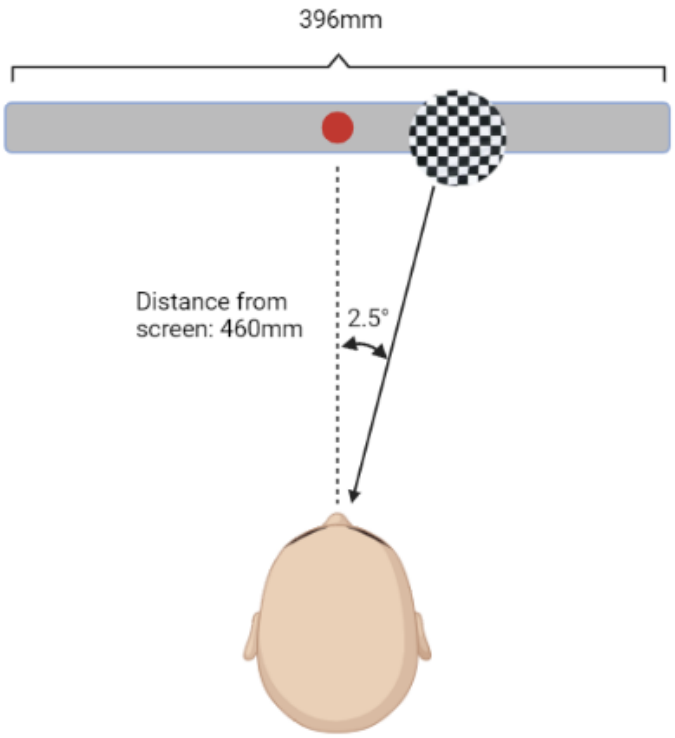

Figure 5: Depiction of the participant task set-up. The script is designed so that the participant sits 46-50cm from the screen with the fixation point positioned at eye level. While the participant is completing the task an EEG is recorded simultaneously, as explained in chapter 3.2 (diagram created with Biorender).

3.1.2 Display and Duration Settings of Task Components

Both tasks featured a fixation point in the form of a red dot in the centre of the screen with a radius of 2.5mm. Circular black and white checkerboards were used as the visual stimuli and presented 2.5 degrees lateral from the visual midline (fixation point) to ensure the stimulus would only present in one visual field for each trial. A black and white checkerboard is usually the preferred choice of visual stimuli in ERP research, because the visual cortex is particularly sensitive to the perception of edges (Odom *et al.*, 2004; Kothari *et al.*, 2014). The checkerboard therefore yields large and reproducible ERP responses on an EEG. Figure 5 shows the section of the MATLAB script responsible for the display properties of the various task components.

The checkerboard stimuli were randomly presented unilaterally to the right or left of the fixation point for a total of 100 trials: 50 to the (RVF) and 50 to the (LVF). Weber et al. found that when participants expected a stimulus in a specific visual field, they tend to covertly allocate their attention to that visual field (Weber *et al.*, 2005). Therefore, it was important that the stimuli were presented randomly so that the participants could not anticipate which visual field would be stimulated for each trial (Weber *et al.*, 2005). A grey scale background was selected to ensure sufficient contrast between the checkerboards and the background and further enhance ERP detection.

```
82      %p.maxTrialFrames=p.fixExpose1+p.fixExpose2+p.startDelay+p.stimExpose+p.textExpose;
83
84 -    p.fullScreen = 1;               %xx fullscreen(1) or windowed (0, useful for debugging)
85 -    p.refreshRate = 60;             % xx refesh rate depends on computer script is run on
86
87 -    p.sf = .6;                      %cycles/deg for checkerboards
88 -    p.tf = 8;                       %temporal frequency (Hz)
89
90 -    p.stimSizeDeg = 10; %xx degrees visual angle of aperture
91 -    p.sx        = [-10,10]; %left right
92 -    p.sy        = [5,5]; %centerish
93 -    p.fixSize =  .4;                %size of fixation square (degrees)
94 -    p.contrast = 1;                 %contrast of checkerboard stimulus
95 -    p.bckGrnd =  .5;
96 -    p.fontColor = 1;
97
98      %stimulus geometry (in degrees)
99 -    p.fixSizeDeg = .25;                % size of the fixation point (radius)
100 -   p.fixColor = [256, 256, 256];      %Color of the fixation point in RGB (white)
101 -   p.textColor=[0 0 0];                %Color of the letters displayed in RGB (black)
102 -   p.fixLineSize = 2;                  % width of the lines that make up the fix point
103 -   p.offsetDeg=2.5; %in deg
104     %---------------------------------------------------------------------------
105     %End user params
106     %---------------------------------------------------------------------------
```

Figure 6: Lines 84-103 of the MATLAB script for the tasks that define the visual properties of the checkerboard, fixation point and letters displayed. The hashed out portions in green define the variables of the corresponding code.

Both versions of the script also contain code responsible for the durations of the various task components including the fixation point, the checkerboard stimuli and the letter displays. These are shown in figure 7 and described in table 3 below.

```
48
49      % number of trials and stimulus duration...
50 -    p.nTrials = 20;                % nTrials/scan, each nTrials consists of a trial + a fix trial
51      %p.sampleOn = .5;               % stim on for this long, then off, then on...
52      %p.stimOn = 1;
53      %p.ITI = .75;
54      %p.nCycles = 1;                 % in stimOnOff cylces (setting this to 1)
55 -    p.startDelay = 0.5; %in seconds
56 -    p.fixExpose1 = 1.5; %in seconds
57 -    p.fixExpose2 = 3; %in seconds
58 -    p.textExpose=0.06; %100 ms
59 -    p.stimExpose=0.06;%50 ms
60      %p.maxTrialFrames=p.fixExpose1+p.fixExpose2+p.startDelay+p.stimExpose+p.textExpose;
```

Figure 7: Lines 50-59 of the MATLAB script that contains variables of the tasks that contributes to the durations of the fixation point, checkerboard, and letter presentation. These are further described in table 3. The "p.nTrails" variable also allowed one to enter how many trials will be displayed for a particular session. This number had to be an even number for equal number of trials for the LVF and RVF.

Table 3: Descriptions of the task MATLAB script parameters that contribute to the durations of the motor task features shown in the MATLAB script (figure 7)

Script parameter	**Descriptions**	**Duration (s)**
p.startDelay	Duration of time between the letter and checkerboard presentation	0.5
p.fixExpose1	Duration of time the fixation point is shown at the beginning of each trail	1.5
p.fixExpose2	Duration of time fixation point is shown at the end of each trial	3.0
p.textExpose	Duration of time the letter (R or P) is shown	0.06
p.stimExpose	Duration of time the checkerboard is shown	0.06

**Time in seconds*

3.1.3 The motor task

The first task involved motor responses. The motor responses did not contribute to the calculation of IHTT but served to assess for attention on the fixation point. As mentioned before, it was important that the participant focused on the fixation point for each trial throughout the task to ensure that only one visual field was stimulated (Banich, 2003; Bourne, 2006). During each trial the fixation point is briefly replaced by a letter “P” or “R” for 60 milliseconds. Three seconds later a beep sound will go off, signalling the participants to press which letter appeared on the screen. The letters “P” and “R” were chosen because they are located on opposite ends of the keyboard, allowing participants to easily press the keys. The two letters also look quite similar upon quick glance, therefore further emphasising that the participants had to pay attention to provide the correct response.

Motor test for each trial:

1. The participant was instructed to focus on the fixation point (red dot) that is displayed for 1.5 seconds at the beginning of each trial.

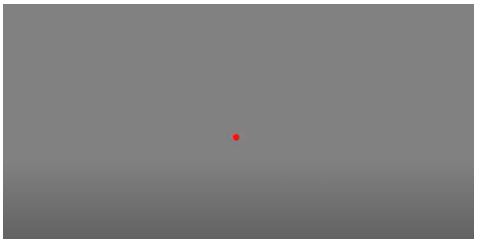

2. The fixation point is replaced by a letter, either a “P” or “R” for 60 milliseconds. The participant was required to remember of the letter presented, because later a beep sound would signal the participant to recall which letter was presented and press the corresponding “R” or “P” on the keyboard.

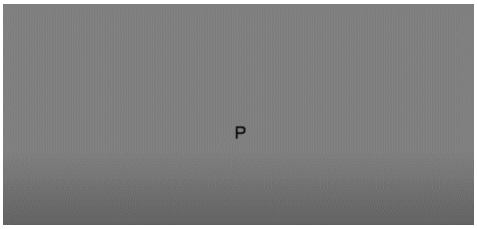

3. 0.5s after letter presentation the checkerboard was presented on the RVF or LVF for 60 milliseconds.

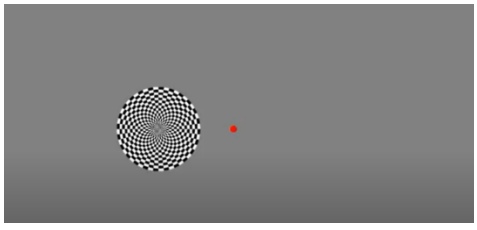

4. 0.5s after the checkerboard presentation a beep will go off, informing the participant to press the letter (R or P) that flashed in step 2 of the trial.

5. At the end of each trial there is a 3 second interval with just the fixation point before the next trial began (step 1).

3.1.4 Non-motor Task

The second IHTT task, namely the non-motor task, is like the motor task in that it features the same fixation point throughout the task and checkerboard stimulus but did not involve the letter presentation and therefore no keyboard motor response. The participant was simply required to focus on the fixation point for the full duration of the task. The main purpose of this task was to serve as an alternative for patients who may have motor difficulties that prevents them from participating in the motor task or if the motor task is too cognitively loaded.

1. The participant was instructed to focus on the fixation point that was displayed for 2s at the start of each trial.

2. The checkerboard was randomly presented for 60 milliseconds to the RVF or LVF.

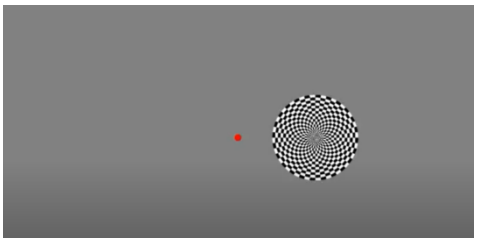

3. There was then a 3.5 second interval with just the fixation point before the next trial (step 1).

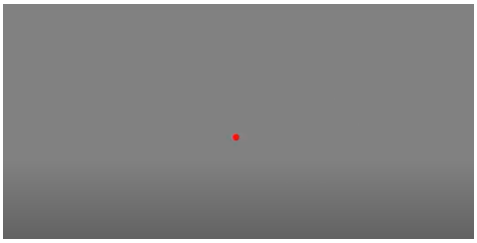

Table 4: Summary of time parameters for the non-motor task

Display	Duration (s)
Fixation point before checkerboard display (step 1)	2.0
Checkerboard Presentation (step 2)	0.06
Fixation point display before next trial (step 3)	3.5

**Time in seconds*

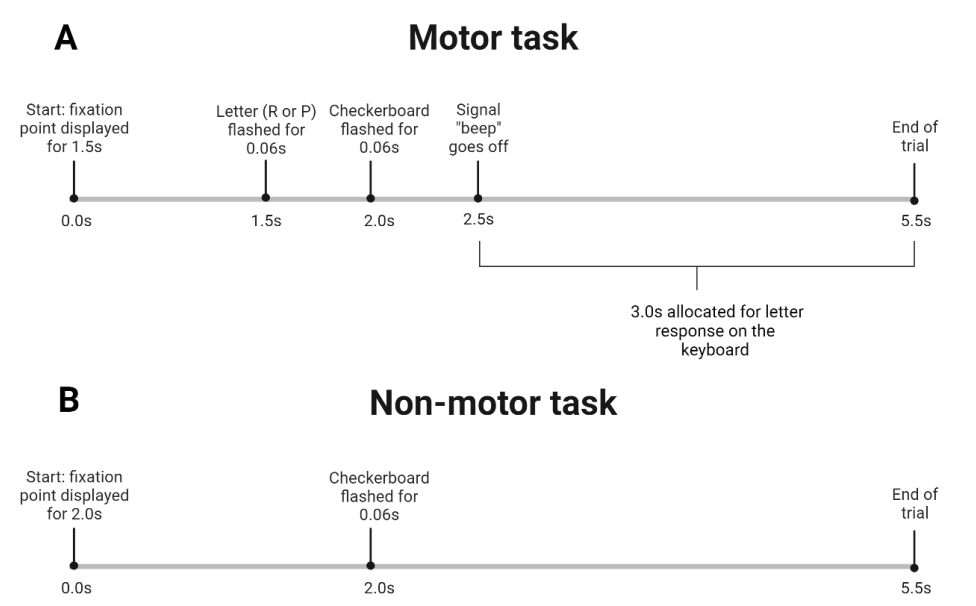

Figure 8: The two diagrams depict the timeline of sequence of events for the motor (A) and non-motor (B) tasks for each trial. Each trial is a duration of 5.5s for both tasks, however the motor tasks also consist of the letter presentation and beep that signals the participant to respond to the with the appropriate keyboard letter response (diagram created with Biorender).

3.1.5 Output Data from MATLAB

The output data provided by MATLAB (figure 9) was used to assess how well participants performed on the motor tasks once they had completed it. This was important for offline EEG analysis. All trials with incorrect responses were removed from EEG averaging, because incorrect responses indicated that the participant was not attentive to the fixation point at the time of checkerboard presentation for a particular trial.

```
           rt: [4.6694 2.2941 3.0101 3.1441 2.9604 3.0598 2.9271 -1]
     randInd: [5 4 2 7 6 3 1 8]
    sameDiff: [128 64 64 128 128 64 64 128]
    possResp: [82 80]
checkFixResp: [82 80]
     letters: 'RP'
      letter: 'PRPRRPPR'
  letterResp: [2 1 2 2 1 2 2 NaN]
     bailout: 27
       space: 32
expStartTime: 2.9936e+06
     correct: [1 1 1 0 1 1 1 0]
  expEndTime: 2.9937e+06
```

Figure 9: An example of output data provided by MATLAB following completion of eight trials of the motor task. Each parameter is further described in table 5. The correct parameter was used for elimination of incorrect trials during the EEG preprocessing stage.

Table 5: Script descriptions for motor task output data

Script Parameter	**Description**
SameDiff	Whether the checkerboard (visual stimulus) was shown on the RVF or LVF.
Letter	The letter shown for that trial (R or P)
letterResp	The letter pressed by the participant - 1: “R”; 2:”P”; NaN: no response
correct	If the participant pressed the correct letter - 0 incorrect or missed; 1: correct

3.2 EEG Recording

An electroencephalogram was recorded with the BIOPAC MP150 (Goleta, CA, US) while the participants completed the tasks, using a waveform and acquisition sampling rate to 500 Hz. A nineteen-electrode cap arranged according to the International 10/20 System (American Encephalographic Society, 1994) was used to record the EEG, along with two ear clips cup electrodes (one on each ear) to ground and the EEG system. Two electro-oculogram (EOG) electrodes were placed near the right eye; one placed 1 cm below the eye and the other 1 cm to the right of the eye to record eye movements. For electrocardiogram (ECG) recording two electrodes were placed on the chest (one on each collar bone) and the third was placed on the right forearm.

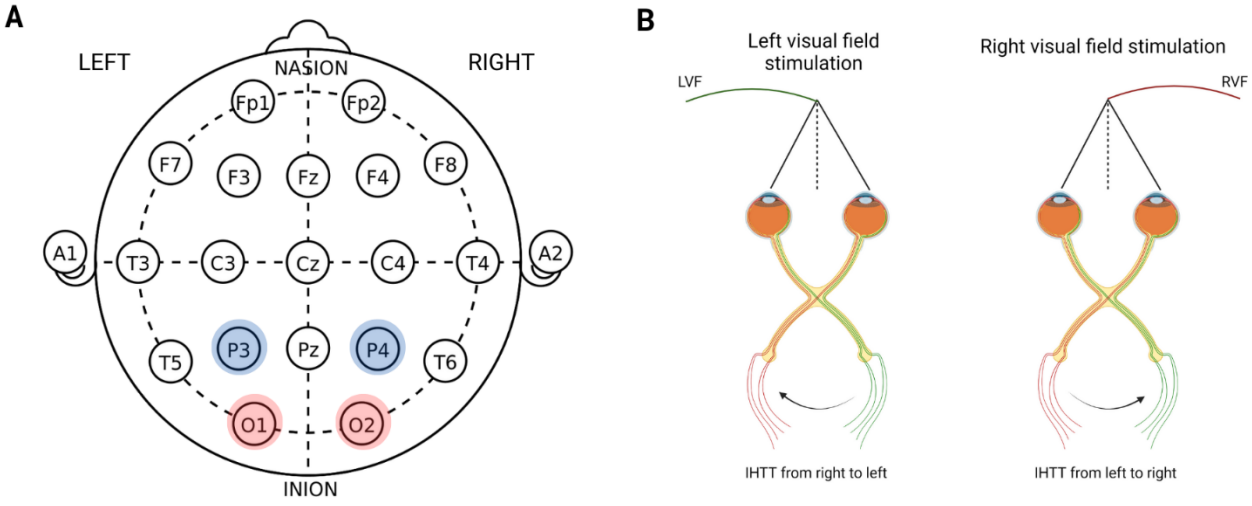

Figure 10: Experimental set up (A) Highlighted EEG electrodes of interest. The parietal sites (P3/P4) and occipital sites (O1/O2) are well described in their use for visual ERP visualisation. P3 and O1 represent the left hemisphere and P2 and O2 represent the right hemisphere. (B) Experimental conditions for the LVF and RVF. All stimuli presented to the LVF will first project in the right (contralateral) hemisphere and then transfer to the left (ipsilateral) hemisphere via the CC. The ERP will occur first in the P4 and O2 electrodes and then in the P3 and O1 electrodes. Similarly, all stimuli presented to the RVF will first project to the left (contralateral) hemisphere and then transfer to the right (ipsilateral) hemisphere via the CC. The ERP will occur first in the P3 and O1 electrodes and then in the P4 and O2 electrodes (diagram created with Biorender).

3.3 Interface between MATLAB presentation laptop and BIOPAC EEG

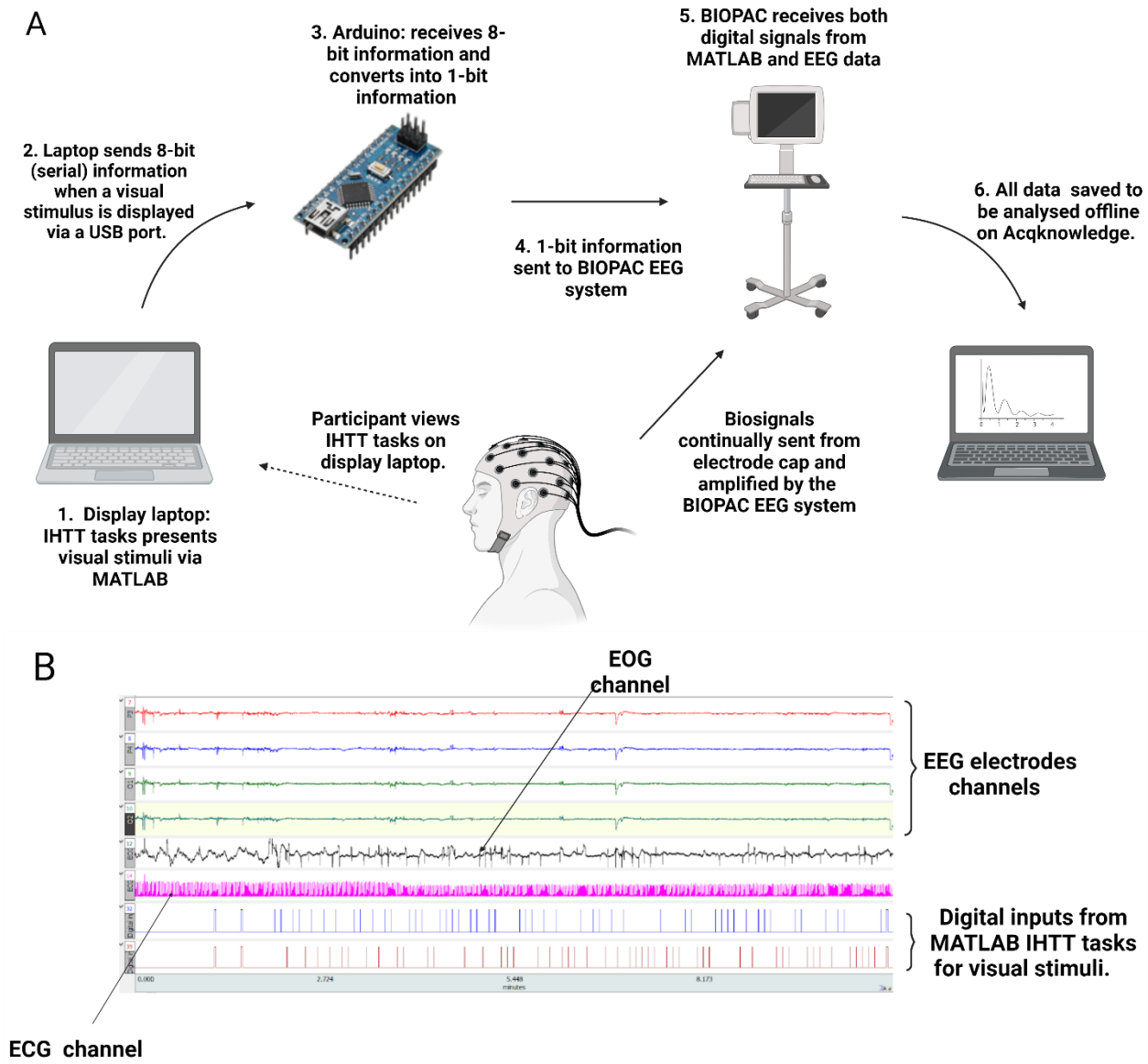

Figure 11: (A) Pathway representing how information from the IHTT tasks and EEG recordings are combined. (B) EEG outputs once task was completed. The parietal and occipital electrode sites were of main interest, which is why those four are highlighted in the figure. The peaks in the last two digital input channels indicates when visual stimulus was presented during the task. Digital input channel 32 (blue) corresponds with stimuli displayed to the RVF and input channel 35 (red) corresponds with stimuli displayed to the LVF (diagram created with Biorender).

An Ardino was connected to the display laptop (via a USB port) and the BIOPAC EEG set up so that constant serial data from MATLAB could be converted to digital signals on the Acqknowledge EEG recording display. The digital signals were outputted on two channels and each peak marks 100 msec before a visual stimulus was displayed during the task. The two channels represented the visual field that was stimulated. As seen in figure 11B the first digital input channel (blue)

displayed all stimuli presented to the RVF and the second digital input channel (red) displayed all stimuli presented to the LVF. This was imperative so that analysis for each visual field could be done separately and offline.

3.4 EEG Pre-processing

EEG pre-processing analysis was done offline to remove trials that did not accurately present in the appropriate visual field. From the MATLAB output data incorrect trials from the motor tasks were noted (as depicted in figure 9 and table 5), because we assume the participant was not focused on the fixation point for that trial and therefore uncertain if the stimulus was displayed in the appropriate visual field. Digital inputs that corresponded with excessive eye blinking and movement artefacts were removed from the raw EEG waveform.

To improve SNR application of an IIR filter with a low band pass of 0.1Hz and high band pass of 50Hz provided the clearest ERPs for both the parietal and occipital sites (Brown and Jeeves, 1993). A study showed that the effects of IIR filters had minimal effects on the latency of ERP components recorded from occipital and parietal electrode sites (Karpiel *et al.*, 2021).

3.5 IHTT Calculation

After the pre-processing steps the “Ensemble Average” function on the Acqknowledge Analysis software (BIOPAC, Goleta, CA) assisted with the offline average process to identify the visual ERPs on the P3, P4, O1 and O2 electrode channels for each visual field – channel 32 for right stimuli and channel 35 for left stimuli. This began by selecting a peak in one of the digital input channels, which would then automatically identify and select all the other peaks in the channel, because they all had the same amplitude. Only 500 milliseconds after the peaks were averaged to allow for appropriate identification of the ERP peaks.

The N1 peak of a visual ERP is described as an uncompounded indicator of IHTT and usually expected to be around 150 msec - 250 msec after the stimulus (Brown and Jeeves, 1993), however with this setup the peaks on the digital channels indicates 100 milliseconds before the stimulus was displayed to the participant, so we expected to identify the N1 peak 250 msec - 350 msec on the averaged electrode waveforms. The N1 peaks were recognised as the most negative peak of the ERP. The latency of the N1 peak for the parietal and occipital waveforms was recorded and stored.

IHTT was calculated by subtracting the latencies recorded by the contralateral electrode from the ipsilateral electrode for each visual field. These latencies were best visualised when the contralateral and ipsilateral waveforms were overlapped. The two IHTTs were then average for an overall IHTT measure from the occipital and parietal electrode each. For example, when calculating IHTT for the RVF, the N1 peak is expected to arrive earlier in the P3 and O1 as they are contralateral to the RVF. The N1 latencies from P3 and O1 averaged waveforms will be subtracted by the P4 and O2 latencies, respectively to end up with two measures of IHTT for the RVF: one from the parietal sites and one from the occipital sites. The IHTT calculation is based on the methods described in Ellis et al 2016. Average IHTTs for each visual field were also calculated for other analysis.

IHTT: RVF = *O2 (RVF) - O1 (RVF) or P4 (RVF) – P3 (RVF)*

IHTT: LVF = O1 (LVF) – O2 (LVF) or (P3 (LVF) – P4 (LVF)

IHTT: occipital = ((O1 (LVF) – O2 (LVF)) + O2 (RVF) - O1 (RVF))/2

IHTT: parietal = ((P3 (LVF) – P4 (LVF)) + P4 (RVF) – P3 (RVF))/2

3.6 Statistical Analysis

The two-way mixed effects model of Intraclass correlation coefficient (ICC) was used to calculate the test-retest reliability for each task and the interrater reliability between the tasks, because we were specifically interested in the reliability of the two IHTT tasks developed for this project (Koo and Li, 2016; Friedrich et al., 2017). The ICC scores were measured separated for IHTTs calculated from the occipital and parietal sites. All correlation statistics were performed on R-Studio (2021). Means and standard deviations of averaged measures were calculated on Excel. ANOVA analysis was used to assess for significant differences between IHTT measured by the RVF and LVF.

3.7 Participants and IHTT Task Testing Procedure

3.7.1 Adult cohort for test-retest reliability analysis

Fourteen healthy students and staff members from the Faculty of Health Sciences (FHS) at the University of Cape Town (UCT) were recruited to be part of the adult reliability cohort. The projected minimum required sample was 11 as calculated in a previous study that also investigated the test-retest reliability of the Poffenberger paradigm (Friedrich et al., 2017). Inclusion criteria included being over the age of eighteen and English speaking. Exclusion criteria included (a) a history of neurological illness, including TBI, stroke, meningitis, and epilepsy, (b) a history of neurodevelopmental disorders and (c) visual difficulties that could not be corrected by glasses or contact lenses. The study was reviewed and approved by the HREC. Approval was also required by UCT's Department of Student Affairs and Human Resources to recruit UCT students and staff. The results of one participant were not included due to poor EEG recordings that prevented the identification of visual ERPs.

Prior to testing, adult participants were required to fill out a COVID-19 screening form before entering the venue to ensure the safety of the lab, the investigators, and other participants. Given that they showed no symptoms and upon entering the test venue participants were instructed to complete a screening questionnaire to collect demographic data and to identify comorbidities that may affect results. The only comorbidity report was depression and anxiety (n=4).

Table 6: Adult cohort profile including median age, sex, handedness, and report of a mood disorder.

Characteristic		**Respondents**
Mean Age (SD)		23.0 (2.42)
Sex	Female	4
	Male	10
Handedness	Right	14
Mood disorder reports		4

3.7.2 Adult cohort testing procedure

Each participant was instructed to be seated in front of the laptop screen according to the set-up shown in figure 6, approximately 46-50cm from the screen. The laptop was also raised to ensure the participant was not slouched throughout the tasks and the fixation point was aligned with the height of the eyes. The motor task was performed first. Participants had an opportunity to practice the task to be familiar with the speed of the letter presentation and as well as the rhythm of

pressing the correct letter after the beep. Once the participants felt comfortable, they were connected to the EEG as explained in chapter 3.3. The motor task was only initiated 1 minute after EEG recording started to stabilise the participant and minimize movement. Participants completed all 100 trials in one session once the motor task began: 50 trials to the RVF and 50 trials to the LVF. Upon completion of the task EEG recording stopped and the data from the motor task was saved.

Once the participant felt ready to complete the second task, a second EEG recording commenced and after a minute of free running EEG the non-motor task was initiated. During preliminary testing of the non-motor task participants consistently reported eyestrain and difficulties in focusing on the fixation point, so the 100 trials were broken up into 3 sessions of 30-40-30 trials to prevent extreme drowsiness. After the third session EEG recording stopped and the data was saved and stored.

Participants returned for a second testing date at least 1 week after the first date to repeat the procedure above, so that we could investigate if results were independent of our EEG set up and examine test-retest reliability for each task.

3.7.3 Paediatric Cohort

A pilot cohort of six pTBI patients were recruited due to the explorative nature of the study. We recruited children who had a previous head injury and were returning for clinical follow-up at the Red Cross War Memorial Children's Hospital (RCWMCH). Inclusion criteria included patients (a) who had sustained a non-penetrating moderate severe TBI, (b) who presented with a GCS of 12 or below, and (c) who were between the age of eight to 12 at IHTT testing. Exclusion criteria included (a) a history of prior neurological illness (including previous TBI, stroke, meningitis, and epilepsy), (b) a previous diagnosis of a neurodevelopmental disorder and (c) visual difficulties that could not be corrected by glasses or contact lenses.

The patients were tested between five to nine months post-injury. Five patients were involved in pedestrian related MVAs, and one was involved in a high-speed velocity MVA. The cohort was evenly split with three moderate TBIs and three severe TBIs. Based on parent self-reports from the clinical notes all patients came from lower socioeconomic backgrounds. The home language of four patients was isiXhosa and Afrikaans for two patients.

Table 7: Demographic and injury details of pTBI cohort.

	Paediatric msTBI cohort
N	6
Age at testing, mean (SD)	8.86 (1.53)
Sex (male)	6 (100%)
Handedness (right-hand dominant)	5 (83%)
Worst GCS score (SD)	8
Time since injury (months, (SD))	7.2 (1.97)
Polytrauma	3 (50%)

Worst GCS score = lowest Glasgow Coma Scale score at scene or arrival at RCWMH if initial GCS score was not available. Polytrauma defined as any other injuries such as orthopaedic trauma sustained in addition to TBI.

3.7.4 Paediatric TBI cohort testing procedure

The testing procedure for the pTBI cohort was very similar to the adult cohort, as explained in chapter 3.2.2; however, the pTBI cohort was invited for only one testing session. The 100 trials for both the motor and non-motor tasks were split into five sessions of 20 trials, so that it would be more manageable for the younger cohort to complete. Before EEG recording the children has sufficient time to practice the motor tasks to ensure each participant could independently perform the task.

Chapter 4: Results

4.1 Feasibility reports for adult test-retest cohort

All (n=14) adult participants were able to complete the full duration of the motor and non-motor tasks for both testing days. One participant's results were not included in the analysis due to unreadable ERP peaks and nodes. The cohort overall was able to provide correct letter responses throughout the motor tasks, with an 98% correct response rate on average. As depicted in table 8 the mean number of incorrect responses was 2/100 reported on the MATLAB outputs report. On average, an additional six trials were removed from analysis due to excessive eye-blinking or movement artefacts. The boxplot in figure 12 shows that the number of trials removed for the motor task are more variable compared to the non-motor task.

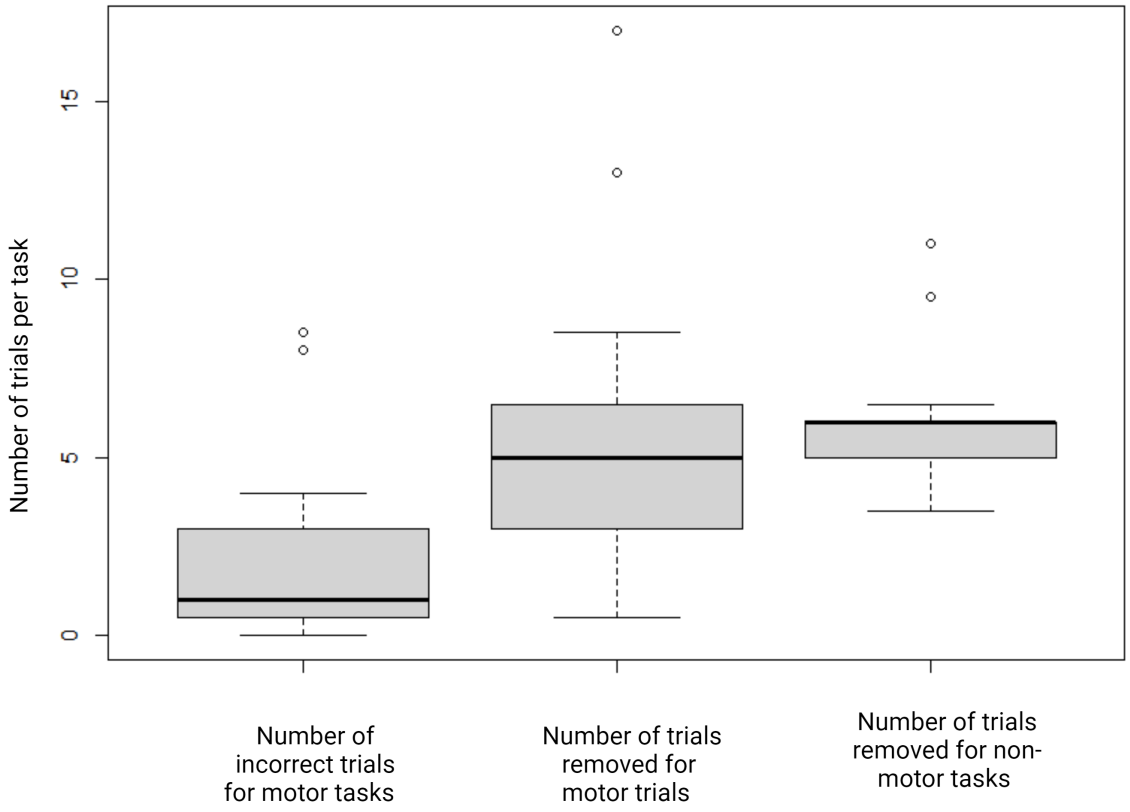

Figure 12: The above box plots displays the number of incorrect trials recorded by the motor tasks, as well as additional trials removed from the motor and non-motor tasks. The number for incorrect trials recorded for the adults were relatively low with a 98% correct response rate in the motor task. The plot also shows that while the correct response rate is high, additional trials still had to be removed due to excessive eye blinking or movement artefacts that could not be corrected for.

Table 8: The mean, minimum, first quartile, median, third quartile and maximum of the average number of incorrect trials for the motor tasks and total number trials removed during EEG pre-processing stages.

	Mean (SD)	Minimum	First quartile	Median	Third Quartile	Maximum*
Incorrect trials for motor tasks	2.27 (2.90)	0	0.5	1.0	3.0	4.0
Trials removed from motor tasks	5.77 (4.72)	0.5	3.0	5.0	6.5	8.5
Trials removed from non-motor tasks	6.00 (2.15)	3.5	5.0	6.0	6.0	6.5

**Maximum outliers excluded on boxplot are included in this table*

4.2 Identification of ERPs and IHTT calculation

Figures 13 and 14 show the ERPs produced by occipital and parietal sites for both motor and non-motor tasks. For the occipital sites the N1 peak latency appears between 340-350 milliseconds after the digital inputs. For latencies for the parietal sites were slightly shorter and variable, detected at 320 milliseconds for the motor task and 280 milliseconds for the non-motor task after the digital inputs. For all four graphs in figures 13 and 14 the ERPs depicted were produced by visual stimuli presented to the RVF. The N1 peaks of the contralateral electrodes (O1 and P3) appear before the ipsilateral electrodes (O2 and P4). IHTT was calculated by latency between the two N1 peaks by subtracting the time of contralateral (O1) N1 peak from the ipsilateral (O2) N1 peak.

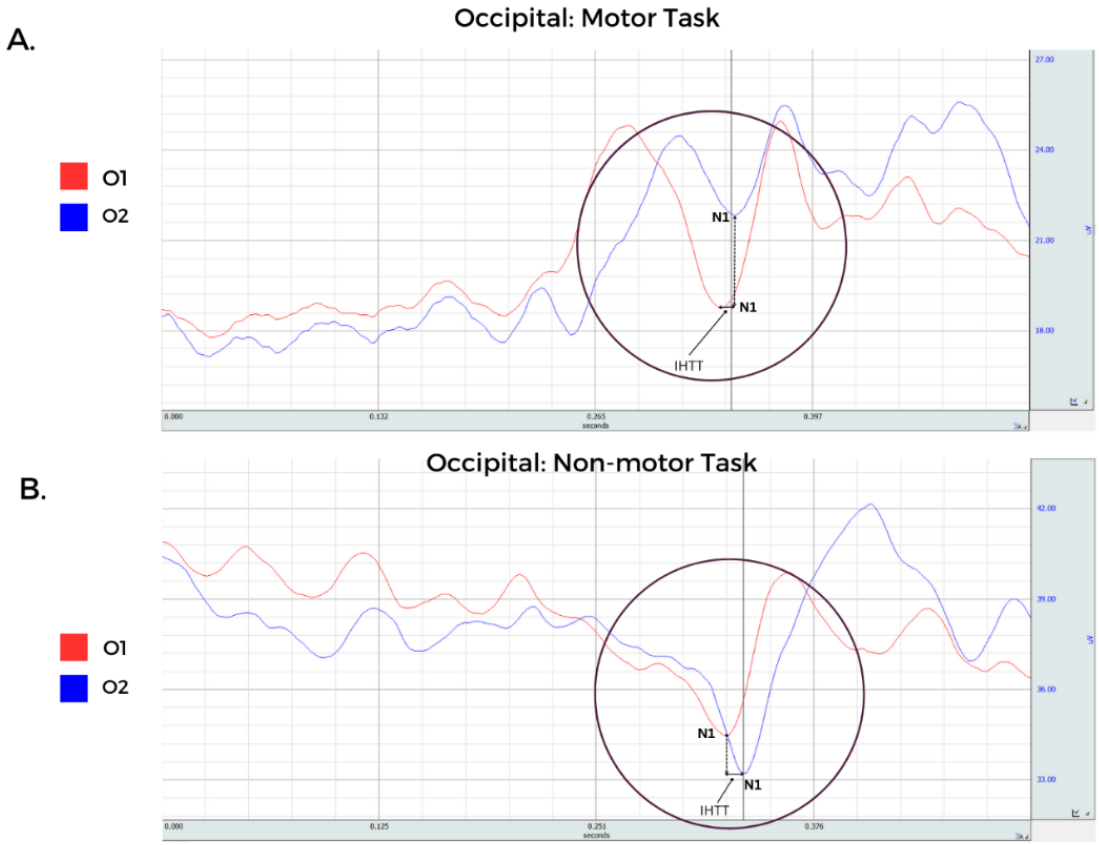

Figure 13: The two graphs depict ERPs produced by the occipital electrodes (O1 and O2) for visual stimuli presented to the RVF. The averaged graphs of the two electrodes were overlapped to visualise the latency between the N1 peaks – recognized as the largest negative peak of the ERP where a clear latency is visible. Graph (A) shows the ERPs produced by the motor task and graph (B) shows produced by the non-motor task. For both tasks the N1 peak appears about 340-350 milliseconds after the digital peak.

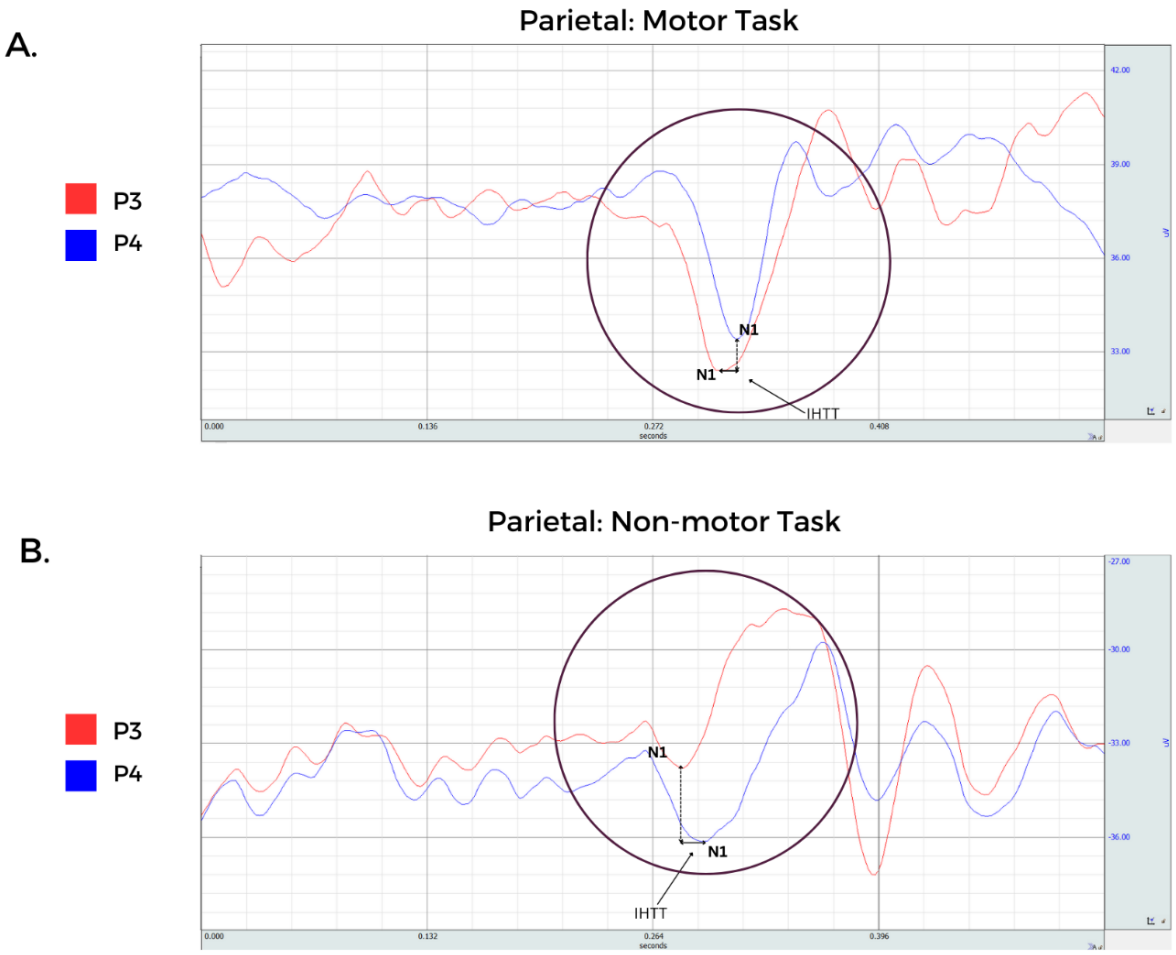

Figure 14: The two graphs depict ERPs produced by the parietal electrodes (P3 and P4) for visual stimuli presented to the RVF. Similarly, to figure 13 graph (A) shows the ERPs produced by the motor task and graph (B) shows produced by the non-motor task. For both tasks the N1 peak appears about 340-350 milliseconds after the digital peak. The N1 latency appears to be shorter, and variable compared to the occipital sites for both task; about 320 milliseconds for the motor task and 280 milliseconds for the non-motor task.

Table 9: Average IHTTs calculated from occipital and parietal sites in the adult cohort.

	IHTT Occipital (ms)		**IHTT Parietal (ms)**	
	RVF	**LVF**	**RVF**	**LVF**
Motor 1	11.7 (3.0)	12.9 (3.5)	11.1 (3.2)	15.8 (4.0)
Non-motor 1	10.6 (3.7)	12.8 (3.2)	12.6 (3.3)	13.7 (2.6)
Motor 2	8.8 (3.7)	11.8 (4.5)	11.7 (2.9)	14.1 (3.9)
Non-motor 2	10.5 (3.1)	12.9 (4.5)	11.8 (4.3)	13.1 (3.2)
Mean Overall IHTT	10.4 (0.5)	12.6 (1.2)	11.8 (1.2)	14.2 (0.6)

**IHTT times recorded in milliseconds.*

Table 9 depicts the average IHTT calculated for the occipital and parietal sites, for each visual field. Even though the IHTTs appear to be longer for the LVF at both occipital and parietal sites there are no significant differences. For the right and left visual field the average IHTTs are about two milliseconds longer for the parietal sites compared to the occipital sites, but these differences are not significant.

4.3 Test-retest and interrater reliability

Test-retest reliability for the motor and non-motor tests were calculated using the Intraclass correlation coefficient (ICC). The two-way mixed effects ICC model was used because the final mean IHTT values were calculated from IHTTs measured for the LVF and RVF. Table 10 shows that IHTTs measured from the occipital electrodes during the motor task provided good test-retest reliability with an ICC = 0.82 where $p<0.005$. The non-motor tasks for the occipital sites provide moderate test-retest reliability with an ICC = of 0.63 where $p<0.05$.

Table 11 shows that ICC values for three out of the four task reliability assessments (motor 1 - non-motor 1, motor 1 – non-motor 2 and motor 2 – non-motor 2) indicated moderate interrater reliability for IHTT recorded at the occipital sites. The motor 2 – non-motor 1 task comparison provided a poor ICC value of 0.29. For IHTT values calculated from the parietal sites both test-retest and interrater reliability ICC values we low were insignificant

Table 10: Test-retest reliability scores for IHTTs calculated from the motor and non-motor tests for both parietal and occipital electrode sites.

	ICC	**p**	**95% Confidence Levels**	
			Lower Bound	**Upper Bound**
IHTTs calculated from occipital sites (O1-O2)				
Motor 1 - Motor 2	0.82	0.0027	0.42	0.95
Non-motor 1 - Non-motor 2	0.63	0.048	-0.206	0.89
IHTTs calculated from parietal sites (P3-P4)				
Motor 1 - Motor 2	0.58	0.072	0.4	0.95
Non-motor 1 - non-motor 2	0.13	0.41	-1.86	0.73

Table 11: Inter-rater reliability scores for IHTTs calculated by the parietal and occipital sites.

	ICC	**p**	**95% Confidence Levels**	
			Lower Bound	**Upper Bound**
IHTTs calculated from occipital sites (O1-O2)				
Motor 1 - Non motor 1	0.68	0.0036	0.266	0.89
Motor 2 - Non-motor 1	0.29	0.28	-1.33	0.78
Motor 1- Non motor 2	0.66	0.039	-0.13	0.89
Motor 2 – Non motor 2	0.69	0.027	-0.081	0.91
IHTTs calculated from parietal sites (P3-P4)				
Motor 1 - Non motor 1	/	/	/	/
Motor 2 - Non-motor 1	/	/	/	/
Motor 1- Non motor 2	0.51	0.12	-0.60	0.85
Motor 2 – Non motor 2	0.20	0.35	-1.62	0.76

4.5 Observational reports on feasibility for paediatric cohort

All pTBI patients (n=6) were able to sit for the full duration of both motor and non-motor tasks. For the motor tasks several practice rounds were required for the patients to familiarise themselves with the keyboard, locate the “P” and “R” letters, and acquaint themselves with the rhythm of the pressing the correct letter at the appropriate time after the beep. Three patients (pTBI1, pTBI3 and pTBI6) would often look up and down between the screen and keyboard during each trial to locate the letters on the keyboard. The other three patients showed minimal difficulty in completing the motor task. All patients (n=6) completed all 100 trials of the non-motor task.

4.6 Number of incorrect scores for pTBI cohort

Across all participants there appeared to be no consistent pattern of practice effects. Overall, the participants did not seem to improve over time, except for pTBI1 and pTBI5. The largest number of incorrect responses was for pTBI1 (46 incorrect responses) where most of these are recorded in the first two sessions. Given the significant decrease in session 3 it is possible that the patient pressed the correct key, but before the beep signal, which is also recorded as an incorrect response.

Table 12: Report on number of incorrect letter responses recorded for each session when pTBI participants completed the motor task.

	pTBI1	pTBI2	pTBI3	pTBI4	pTBI5	pTBI6
Session 1	18	2	7	0	3	4
Session 2	20	1	1	0	1	0
Session 3	3	2	1	1	0	4
Session 4	1	3	5	1	0	0
Session 5	4	5	2	0	0	0
Total	46	13	16	2	4	8

4.7 Identification of ERPs and IHTT calculation for pTBI cohort

For the pTBI cohort, IHTTs were only measured from ERPs identified from the averaged occipital waveforms, given that the test-retest and inter-rater ICC scores were low for the parietal electrode sites. Figure 15 displays the overlapped waveforms of the O1 and O2 electrodes. Similar to the adult cohort, the N1 peak of the ERPs are identified after the 300-millisecond mark for both tasks. Figure 15A represents waveforms from the motor task for stimuli presented to the RVF. At the marked ERPs the N1 peak of the O1 arrives before the O2, as expected given that O1 is situated on the left hemisphere, representing the contralateral condition for the RVF. Figure 15b represents waveforms from the non-motor task for stimuli presented to the LVF, where the N1 peak of the O2 electrode arrived earlier than that of the O1. The IHTT was calculated from the latencies between the N1 peaks of the contralateral and ipsilateral electrode sites.

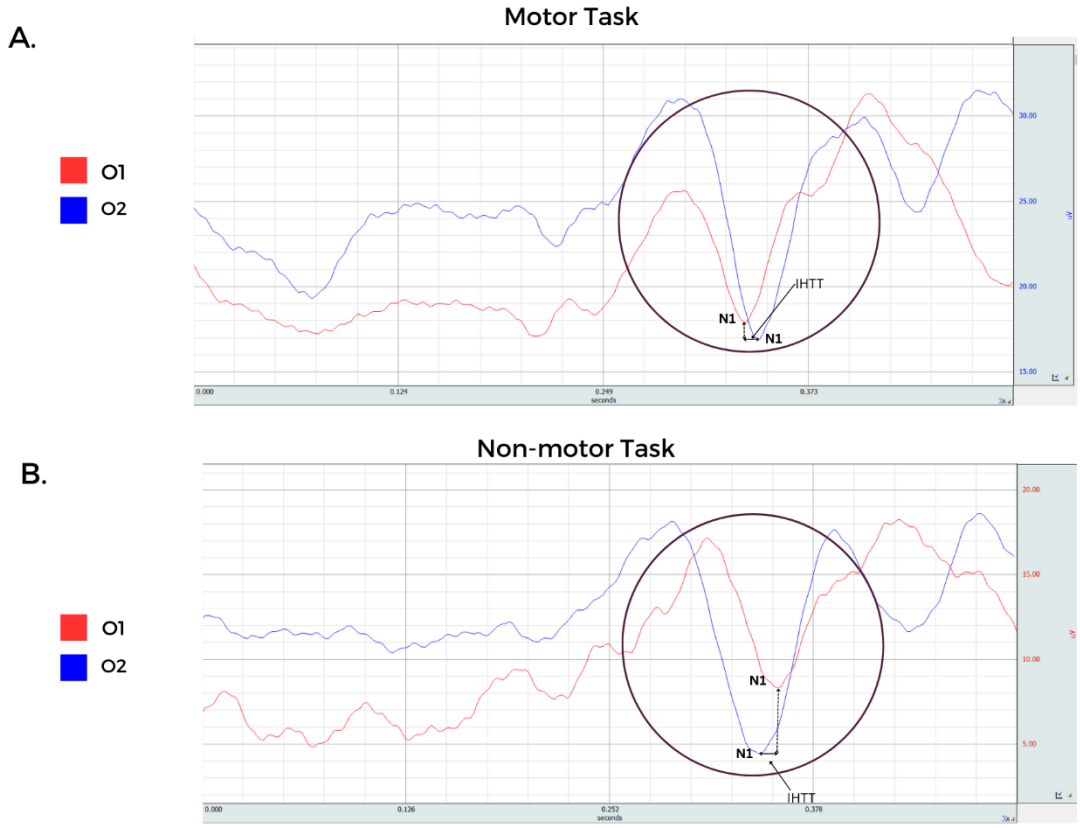

Figure 15: The two graphs represent averaged and overlapped O1-O2 channels for the digital inputs from the IHTT tasks performed by the pTBI cohort. The red graph represents the O1 channel, and the blue graph represents the O2 channel. (A) Overlapped occipital channels when the participant performed the motor task for the RVF. (B) Overlapped occipital electrode channels from the non-motor task for the LVF.

Table 13: Calculated IHTTs for each visual field using waveforms from the O1-O2 electrodes sites for motor and non-motor tasks.

	Motor (ms)		Non-motor (ms)	
	RVF	**LVF**	**RVF**	**LVF**
pTBI1	-	-	10.0	6.0
pTBI2	12.0	10.0	8.0	-
pTBI3	-	-	14.0	16.0
pTBI4	10.0	8.0	6.0	10.0
pTBI5	-	8.0	8.0	10.0
pTBI6	-	-	8.0	18.0
Mean (SD)	11.0 (1.4)	8.7 (1.2)	9.0 (2.8)	12.0 (4.9)

Table 13 shows that even though all pTBI completed the motor task, IHTT could not be calculated for patients pTBI1, pTBI3 and pTBI6 for both visual fields. For pTBI1 this was due to nearly 50%

of the trials having incorrect motor responses. For patients pTBI3 and pTBI6, ERPs could not be reliably detected due to excessive movement throughout the EEG recording. In patient pTBI5 IHTT could only be calculated for the LVF.

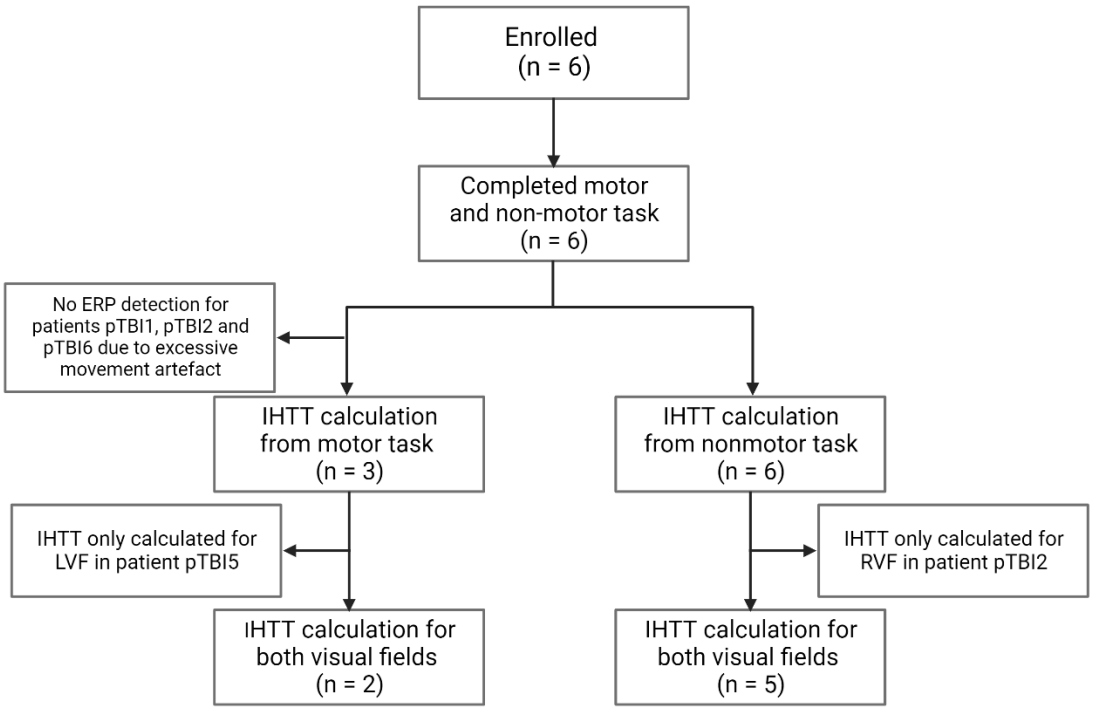

Figure 16: Study cohort for the pTBI patients – summary on task performance and IHTT calculations for the pTBI group.

For 5 of the patients (83%) IHTT could be calculated from the non-motor tasks for both visual fields. It is interesting to note that the mean IHTTs calculated for the pTBI were similar and slightly shorter compared to those calculated for the healthy adult cohort at the occipital electrode times; however, the differences between adult and paediatric anatomy and physiology must be considered in interpreting this. The adult cohort had a IHTT mean of 11.5 milliseconds and the pTBI cohorts had a mean of 9.85 milliseconds.

Chapter 5: Discussion

This study aimed to assess whether two locally developed IHTT tasks were (1) feasible to perform in healthy adults and a cohort of children with previous TBI, (2) effective in producing visual ERPs on an EEG and (3) if the two tasks provided reliable measures for interhemispheric transfer time. A quantitative and observational approach was used for the assessment of the two tasks.

5.1 Feasibility and ERP of IHTT tasks in adult cohort

When developing the tasks, there were concerns that 60 milliseconds for the letter presentation of “P” or “R” during the motor task might be too fast for accurate responses, especially for the pTBI cohort. In the adult cohort we found that on average only two incorrect trials out of the 100 were recorded, which was a satisfactory response. The tasks are based on the divided field technique that required the participants to focus on the fixation point to ensure the visual stimuli were presented in the appropriate visual field. The main purpose of the keyboard letter response was to check that the participant remained focused on the fixation point for each trial. The quick display of the letter in place of the fixation point and the low percentage of incorrect trials recorded indicates that not only does motor response serves as an appropriate method to control for attention, but that the adults were able to remain focused for the full duration of the task.

During preliminary assessments of the non-motor task, participants reported eyestrain and difficulty paying attention on the fixation point for the full duration of the 100 trials. Therefore, the trials were divided into three sessions of 30-40-30, allowing for rest during the session and better attention during the tasks. Based on the literature, this project presents one of the first visual ERP-based methods that makes use of a simple non-motor task. Auditory ERPs have been used to assess for cognitive impairments; however few studies have validated an auditory ERP method for measuring IHTT.

The limitation with the non-motor task is the lack of objective measure to assess if the participant was focused on the fixation point. Even though we made use of information from the EOG electrodes and observational records, it cannot be as accurate as the motor task in measuring attention. The EOG data was helpful in removed trials that coincided with excessive eye blinking but does not account from slight deviations from the fixation point while participant’s eyes were open for a particular trial.

5.2 Parietal vs occipital measures of interhemispheric transfer time

While we were able to identify visual ERPs at the P3/P4 electrode sites, the IHTTs calculated from these sites provided poor ICC values when compared with IHTTs measured from the O1/O2 electrode sites for both the motor and non-motor task, suggesting that it may not be appropriate to interchangeably use IHTT measures from different pairs of electrodes and that the occipital lobes provide better ERPs for visual stimulation. This was surprising considering that other electrophysiological studies investigating IHTT made use of P3/P4 and even C3/C4 for IHTT estimations (Brown and Jeeves, 1993; Brown *et al.*, 1999; Ellis *et al.*, 2016; Chaumillon, Blouin and Guillaume, 2018). Ellis et al. (2016) calculated IHTT by averaging IHTTs measures from both the parietal and occipital electrodes, or in case where ERPs were not identified by the occipital sites, IHTTs calculated at the parietal sites were used instead. Possibly it may have been more appropriate to report IHTT measures for each pair of electrodes, instead of averaging the 2x2 combination for an overall averaged IHTT.

Chaumillion et al. (2018) further highlighted the importance of reporting IHTTs measured from pairs of electrodes separately. They found significantly shorter IHTTs measured at the central (C3/C4) sites compared to those measured at the parietal (P3/P4) sites (Chaumillon, Blouin and Guillaume, 2018). The transfer of information from the sensorimotor cortices can be used to calculate IHTT from the central sites, however tasks designed to produce ERPs with visual responses typically do not use the central electrode sites to calculate IHTT, provided that visual information is first received in the occipital lobes. Given that the non-motor task does not involve the sensorimotor cortices, it further highlights that it would not have been appropriate for this study.

Several studies investigating EEG electrode placement variability in the 10-20 and 10-10 system reported that the parietal and occipital lobes present with the highest electrode position variability across participants (Okamoto *et al.*, 2004; Atcherson *et al.*, 2007; Koessler *et al.*, 2009; Scrivener and Reader, 2022). These same patterns of deviations and variability are consistent with studies that used manually placed electrodes and electrode caps (Atcherson *et al.*, 2007). Despite electrode position variability, Koesller et al. (2009) observed that O1 and O2 always projected to the secondary visual cortex and the cuneus in the same proportions (Koessler *et al.*, 2009). Considering that the secondary visual cortex and cuneus make up the bulk volume of the occipital lobe and are responsible for the early processing of visual information, it may be more appropriate to rely on IHTT measured visual ERPs detected by occipital electrode sites. On the contrary, they

observed more variability in the parietal sites where P3 and P4 projected to Brodmann areas 39, 40, 7, 37 and 19. Scrivener and Reader (2022) also found that projections to the P3/P4 mainly came from the angular gyrus that is involved in more complex language-related functions and social cognition (Seghier, 2013; Scrivener and Reader, 2022). These studies further suggest that it is not appropriate to use IHTT measures interchangeably. In the context of this study, it may be appropriate to use the P3/P4 sites considering the visual ERPs are produced by very simple IHTT tasks.

The variability in electrode position also suggests that there needs to be caution in assuming each electrode projects to the correct corresponding underlying brain region. It is important to note that scalp recordings from an EEG do not exclusively represent activity from the closest region of the underlying cortex; however, researchers generally select specific electrodes for analysis based on their proximity to a particular area. More data are needed on the variability of IHTTs measured by different pairs of electrodes, and which pairs provides better test-retest reliability.

5.3 Test-retest and interrater reliability of IHTT measures

The test-retest reliability IHTTs measured from the occipital sites for the motor-test provided an ICC of 0.82 which is considered good reliability and suggest that IHTTs measured by the motor task were independent of the set-up. Friedrich et al. (2017) were one of the few studies to report the long-term reliability of an EEG-based IHTT task. Similarly, they reported a high positive correlation of 0.81 for the test-retest reliability to their motor EEG-based IHTT task; however, they used the Pearson Correlation Coefficient to assess for reliability (Friedrich *et al.*, 2017). Pearson correlations may be misleading in judging agreement because while both the ICC and Pearson Correlation Coefficient examines the degree of relationship between datasets, ICC examines absolute agreement between datasets and Pearson examines linear correlation (Liu *et al.*, 2016). For test-retest reliability there needs to be certainty that each task provided similar IHTT values for both testing sessions, and therefore using ICC to assess for test-retest reliability may be more appropriate.

The non-motor task had a moderate test-retest reliability of 0.63. This may indicate that the non-motor is more sensitive to factors such as the lighting in the room and inattention in the non-motor tasks. No other study has reported test-reliability for a non-motor ERP task and therefore difficult to deduce if an ICC score of 0.63 is unusually low or expected for these kinds of tasks.

Three ICC values for interrater reliability between the motor and non-motor task were also moderate, ranging between 0.62 and 0.69. Again, it is difficult to appropriately assess how these scores compare to the literature given this study is the first study to investigate the interrater reliability between two EEG-based IHTT tasks. This lower moderate reliability may also reflect that the sample was too small for assessment or there was a lack of variability among the sample (Müller and Büttner, 1994). Given that the minimum sample required for this study was 11 (Friedrich *et al.*, 2017), the sample size may not be the problem and suggests we need more data on test-retest reliability of tasks used for investigating IHTT.

5.4 EEG IHTT measures compared with previous studies.

This study reported IHTT values that ranged from (10ms-14ms) from the O1/O2 and P3/P4 pairs of electrodes. These fall in the range of IHTT measured by other studies, where IHTTs measures by EEG methods report values between eight and 30ms (Westerhausen *et al.*, 2006; Friedrich *et al.*, 2017; Chaumillon, Blouin and Guillaume, 2018). Westerhausen et al. (2006) measured IHTT from P3/P4, O1/O2 and T5/T6 from the P1 and N1 components of the ERPs and calculated IHTTs that ranged between 8.1-18.9 milliseconds. Friedrich et al measured only measured IHTT from occipital sites with an average of 15.4ms and wide range of 2.6-18ms. Chaumillion et al. (2018) calculated shorter IHTT values at the central sites compared to those measured from the parietal sites. They measured IHTT values as short as 5.3ms at the central sites and other measures as long as 29.4ms at the parietal sites. The literature reports that more anterior sites provide shorter IHTT measures (Ipata *et al.*, 1997; Chaumillon, Blouin and Guillaume, 2018). This was not reflected in this study where no significant differences between IHTTs measured the occipital and parietal sites were reported. In comparing the IHTT values to other studies, the patient status (healthy/ disease) and age must be considered.

5.5 Detection of asymmetries in IHTT

Chaumillion et al. (2017) reported asymmetries in IHTT based on handedness - right handers with right eye-dominance showed faster transfer from left to right hemisphere and vice versa in participants with left eye-dominance. However, in our study even though it appeared that IHTT values measured for the RVF were faster in the adult population at both the occipital and parietal sites, these differences were not significant. It is not clear why no differences were detected in our cohort; possibly because of the small sample size. However, there are notable methodological differences where Chaumillion et al compared right- and left-handed participants and broke those groups further down into subgroups of right or left eye dominance.

We also did not observe any asymmetries in IHTT in the pTBI cohort, similar to Ellis et al. (2016), where they found no differences in IHTTs measured for the LVF compared to the RVF. Given that white matter is a protracted phenomenon it is possible that these patterns of asymmetry are only established in adults where the corpus callosum is fully developed (Muetzel et al., 2008; Chevalier et al., 2015). The lack of significant differences between LVF and RVF IHTTs for the pTBI cohorts also suggests that it may be appropriate to average the IHTT values to calculate an overall IHTT measure for children. This lack of difference should be further examined in larger cohorts, with the inclusion of normal control participants for comparison.

5.6 Feasibility reports in children

5.6.1 Difficulties with assessment in the motor task

All participants were able to complete full 100 trials of the motor tasks, however, as discussed in the results IHTTs could not be calculated for both visuals fields. For pTBI1 almost 50% of the recorded letter responses were incorrect, where most of the incorrect responses were recorded in the first two test sessions. Given the improvement in the session 3 it is possible some responses in the previous two sessions where correct, but the participant responded too quickly following the letter presentation and did not wait for the beep sound that signals when a participant should press the key. It was also observed that pTBI1, pTBI3 and pTBI6 were constantly moving their heads between the laptop screen and the keyboard in efforts to not forget the letter that was presented and immediately press on the keyboard. With the constant moving up and down we are therefore not certain if participant was focused on the screen while the visual stimuli were presented. This is further reflected in the results where IHTTs for patients pTBI1, pTBI3 and pTBI6 could not be measured from the motor tasks due to unreliable ERP detection.

The literature shows that pTBI children that suffered a severe injury disproportionately perform poorer on visual reaction time tasks (Mathias *et al.*, 2004; Catroppa *et al.*, 2008; Jonsson *et al.*, 2013). The three patients highlighted earlier (pTBI1, pTBI3 and pTBI6) all had low initial GCS scores, so it was not surprising to observe that the constant head movements and slight difficulty in performing the tasks were observed in those three participants. The act of looking down immediately may also reflect impaired working memory (Gorman *et al.*, 2017; Phillips *et al.*, 2017). Their efforts to immediate locate the letter on the keyboard may indicate how unfamiliar they are with a keyboard and efforts to not forget. The clinical notes do note that all these patients in the study come from low-middle socioeconomic backgrounds where it is likely this study was the first time they interacted with a keyboard. Patients who sustain TBI often come from poorer socio-

economic backgrounds, and post-TBI behavioural difficulties (especially attentional deficits) are common and are expected to interfere with the ability to attend to instruction.

5.6.2 Feasibility and ERP detection in non-motor tasks

All patients were able to complete the full 100 trials of the non-motor task. We were surprised to observe that it was easier to identify ERPs and calculate IHTT in the non-motor task, considering that the highest ICC score for adult cohorts was recorded for the motor task. Initially we anticipated it would be more challenging for the patients to be attentive for the full duration of the non-motor task given that the adult cohort reported it was more difficult to complete the non-motor task compared to the motor task. However, it must be noted for the pTBI participants, the 100 trials were split in five sessions of 20 trials that allowed for more rest, compared to the 30-40-30 trial sessions in the adult cohort.

Overall, fewer head movements were observed when the patients completed the non-motor task compared to when they completed the motor tasks. The reduced movement artefact allowed for fewer trials to be removed from analysis and better ERP identification to assist with IHTT calculation. This also indicates that perhaps the complexity of the motor task was underestimated and that improvements in the set-up could facilitate easier responses for the pTBI patients and better ERP productions. For example, the use of a chin rest may assist in minimizing head movements and the use of a joystick instead of keyboard responses may help gamify the task.

5.7 Comparison of IHTT values to other pTBI cohorts and adults

The IHTT measures from the pTBI cohort appear in keeping with values from other studies. Our mean IHTTs ranged from 8.7ms to 12.00ms. Also in children, Dennis et al calculated a mean of 9.27ms in their pTBI-normal group and a mean of 25.31ms in their pTBI-slow group. Ellis et al calculated a mean of 8ms in their pTBI-normal group and 25.9ms in their pTBI-slow group. The wide range between normal and slow IHTTs within one moderate-severe cohort suggest that severity is not always indicative of functional outcomes (Lieh-Lai *et al.*, 1992). Contrary to our findings Meisner et al found that seven-year-olds had significantly slower IHTT times compared to the adults. The authors suggested that IHTT could also serve as a tool to investigate the functional development of the CC from childhood to adulthood (Meissner *et al.*, 2017). The lack of significant differences between our adult and child cohort could reflect the exploratory nature of the study and the relatively small cohort sizes.

5.8 pTBI in the South African context

Although the cohort is small, it does reflect the demographic profile for moderate-severe pTBI population observed at RCWMCH. According to Schrieff et al (2013) at RCWMCH vast majority of children admitted for moderate or severe TBIs are males, and this is similarly observed globally (Schrieff *et al.*, 2013; Dewan *et al.*, 2016b; Thurman, 2016). It is likely that this is related to some of the behavioural differences observed in boys, making them more vulnerable sustaining a TBI (Schrieff *et al.*, 2013). Furthermore, the peak age for these MVA-related TBIs is six years old (Schrieff *et al.*, 2013) that compares reasonably with the mean age of eight for participants in this study. This is younger compared to other studies investigating IHTT where their paediatric cohorts include adolescent patients up to the age of 18. Ellis et al. (2016) had a mean age of 14.5 years for their pTBI cohort, Benavidez et al had a mean of 12 years and Dennis et al. had a mean of 14 years at testing. These age differences are important because the physiology and injury characteristics of children and adolescents differ. Furthermore, the logistics and likely success of performing instructed tests like the IHTT differ with age, with completion in younger patients likely being more difficult. Arguably though, the value in younger patients may be greater because the developmental trajectory is steeper and school-based assessment of baseline cognitive functioning is less likely to be available. The developmental level of the child at the injury is often a predictor of outcome in educational and functional areas (Catroppa and Anderson, 2006; Catroppa *et al.*, 2008; Jonsson *et al.*, 2013). Therefore, having an objective physiological measure of processing speed would be valuable.

Lastly, there are significant positive correlations between age and WM development and so it might not be appropriate to compare IHTT measures from eight-year-olds with older adolescent cohorts (Muetzel *et al.*, 2008; Kochunov *et al.*, 2012). This study presents as one of the few studies to include a young pTBI cohort and highlights the overall need for the young pTBI population to be included in research and to develop more appropriate tasks for testing.

Given that this study also took place in the context of South Africa we also need to recognize the challenges that comes with testing in a cohort like this. Most of these children come from low-middle socioeconomic backgrounds, where finding transport to be at test venue, clinic for follow up is a great challenge. It is important to identify these factors because they also contribute to the recovery of a child post-injury and there are other challenges associated with performing and conducting these sorts of testing in children. Performing neuropsychological batteries is also a challenge because they are time-consuming, and appointments for neurodevelopmental clinics

within the public sector have long waiting lists. More important, many standard neuropsychological tests have not been validated for the diverse South African population. The potential predictive value of these IHTT tasks may be an affordable alternative to neuropsychological tests when they are not available.

5.9 Limitations

5.9.1 Lack of objective measure for attention in non-motor task

While the non-motor task was able to produce large, identifiable ERPs, a more objective method is necessary to ensure participants are focused on the fixation point so that the visual stimuli are presented in the appropriate visual field. A solution may be to use an eye-tracking system that is calibrated with EEG recording to ensure that the focus on the fixation point corresponds with the presentation of each stimulus, and appropriately exclude from downstream analysis those that do not. Eye-tracking may allow also for better correction and accommodation of eye movement artefacts (Scharinger, Schüler and Gerjets, 2020).

5.9.2 Low number of trials for ERP averaging

The tasks were designed to be as short as possible to accommodate the attention span of a young pTBI population. This unfortunately led to a low number of trials to average for ERP visualization. Both tasks had a high of 50 trials for each visual field, however in the case of all participants less than 50 trials were average due to either incorrect trials, eye-blinks, or excessive movement artefacts. This was particularly noticeable in the pTBI cohort where IHTT could not be measured from the motor tasks in three participants due to a large number of incorrect trials and/or excessive movement. The removable of 20 or move trials affected the ability to reliably identify ERPs. Fifty trials per visual field is also considerable low compared to other ERP-IHTT studies. Others have used larger numbers of trials: Chaumillion et al (500 trials), Ellis et al. (388 trials), Westerhausen et al (300 trials) and Friedrich et al (300 trials) – all for each visual field (Westerhausen *et al.*, 2006; Ellis *et al.*, 2016; Friedrich *et al.*, 2017; Chaumillon, Blouin and Guillaume, 2018). More trials may have controlled for large numbers of incorrect trials or movement artefacts. For the adult cohort a greater number of trials could have also facilitated the production of larger ERPs at the parietal sites and higher ICC values for test-retest and interrater reliability. That said, using a large number of trials in this population group likely would be difficult, not only because they are children, but also because most will likely have a cognitive and/or behavioural disturbance. Furthermore, the population of children who are accidently injured may well have a higher

incidence of permorbid behavioural disturbances (such as hyperactivity and impulsivity) that placed them at higher risk of injury in the community.

5.9.3 Homogenous adult and pTBI cohorts

The adult and pTBI cohorts were majority males, where 100% of patients recruited for the pTBI cohort were male. Considering that boys are more likely to be involved in a TBI is not surprising that more males were recruited but for research purposes it would have been more appropriate to include more female participants, particularly for the feasibility observational reports for the IHTT tasks. This is a pilot project to assess the technical logistics of performing these tests, however. To evaluate the performance of the test as a measure of functional outcome would require a larger and more diverse sample.

5.10 Future Research

The results of the present study, and our experience acquired during the project, show that the setup and tasks were able to produce ERPs and measure IHTT but could be improved by adaptations in the task and EEG set-up. These include presenting the tasks in a more dimly set room, using a higher EEG samples rate for EEG acquisition, and increasing the number of trials to accommodate for more movement artefacts and eye-movement (subject to participant tolerance). Using an eye-tracking device in combination with the EEG recording may also serve as way to control for attention in the non-motor task. ‘Gamifying’ the system, for example by using a joystick instead of keys, may improve performance in the motor task requirements.

Recruiting a control group of participants of similar age and background would be helpful in interpreting the results. Recruiting a larger patient sample would also allow one to further investigate the reliability of these two tasks by introducing more variability within the sample. This would help assess whether the moderate reliability scores calculated for this study are due to limitations of using the ICC or if the task itself is only moderately reliable. Comparing the results with functional measures of short- and long-term outcome, as well as with other potential biomarkers of injury and recovery, such as advanced MRI metrics, is necessary to determine the predictive value of the test in young patients. It would be interesting to note if the IHTT measures for this cohort holds a similar predictive value compared what Ellis et al (2016) observed. PTBI children with normal IHTTs performed better on neurocognitive assessments compared to those with slow IHTTs (Ellis *et al.*, 2016). At two years following injury, recovery is usually stabilized

(Van Heugten et al., 2006),so it would be interesting to compare IHTTs measured during the subacute phase and two years following injury and the degree of recovery.
Currently there is limited literature available on advanced MRI analysis on South African pTBI cohorts, however, data in this field are being collected. It would be useful to compare the IHTT measures with structural outcomes for the South African pTBI population, as noted on various MRI modalities such as volumetric analysis from structural images and WM integrity as measured by DTI analysis (Dennis *et al.*, 2015, 2017).

Lastly, these ERP-IHTT tasks could also be used to investigate the functional development of the CC between different child age groups. To date only two studies have investigated IHTT between child age groups and only made use of behavioural reaction time tasks to measure IHTT, where they have found that younger children tend to have longer IHTTs compared to older and adolescent children (O'Leary, 1980; Brizzolara *et al.*, 1994). These behavioural studies are difficult to compare because the longer reaction times in younger children could also reflect difficulty in performing the tasks and underestimates the complex visuomotor pathways involved in performing reaction time tasks (Ratinckx, 1997). It would be more appropriate to investigate CC functional development using electrophysiological methods for calculated IHTT.

Chapter 6: Final Conclusions

The study is one of few to investigate IHTT in a young pTBI cohort using visual ERPs and one of the first to develop a task that does not involve motor responses. The study found that these simple tasks effectively produced ERPs for both adult and paediatric cohorts and calculation of IHTT measures that fell in the range of IHTT measures from previous studies. Even though the results imply the motor task offers high test-retest reliability, it was more appropriate to calculate IHTT from the non-motor tasks for the paediatric cohort. This suggest that further investigation is required to improve the testing conditions to improve the reliability scores or to further gamify the motor task for the younger cohort. This study also provides evidence that EEG electrode sites for IHTT should be selected with caution, as indicated by the lower ICC scores provided by IHTT measures from the parietal sites.

Measuring IHTT to assess the WM integrity seems to be a promising tool and cheaper alternative to predict functional outcomes within a pTBI cohort. Even though this study only features a pilot pTBI cohort the outcomes are promising as a tool that can be used for younger TBI cohorts. However, the true predictive value of these tasks can only be measured by comparing the IHTT measures with neurocognitive performances, as well as how they compare to children with no history of a head injury. Further longitudinal investigations may also look at if there are changes in IHTT measures overtime and if it is indicative of normal CC development or CC atrophy.

References

Allen, D.N. *et al.* (2010) 'Memory and attention profiles in pediatric traumatic brain injury', *Archives of Clinical Neuropsychology*, 25(7), pp. 618–633. Available at: https://doi.org/10.1093/arclin/acq051.

Angelova, P. *et al.* (2021) 'Contemporary insight into diffuse axonal injury', *Folia medica*. Available at: https://doi.org/10.3897/folmed.63.e53709.

Anzola, G.P. *et al.* (1977) *SPATIAL COMPATIBILITY AND ANATOMICAL FACTORS IN SIMPLE AND CHOICE REACTION TIME*, *Neuropsychologia*. Pergamon Press. Printed in England.

Ashwal, S. *et al.* (2000) 'Predictive value of proton magnetic resonance spectroscopy in pediatric closed head injury', *Pediatric Neurology*, 23(2), pp. 114–125. Available at: https://doi.org/10.1016/S0887-8994(00)00176-4.

Ashwal, S. *et al.* (2006) 'Susceptibility-Weighted Imaging and Proton Magnetic Resonance Spectroscopy in Assessment of Outcome After Pediatric Traumatic Brain Injury', *Archives of Physical Medicine and Rehabilitation*, 87(12), pp. 50–58. Available at: https://doi.org/10.1016/j.apmr.2006.07.275.

Atcherson, S.R. *et al.* (2007) 'Variability of electrode positions using electrode caps', *Brain Topography*, 20(2), pp. 105–111. Available at: https://doi.org/10.1007/s10548-007-0036-z.

Babikian, T. *et al.* (2011) 'The UCLA Longitudinal Study of Neurocognitive Outcomes Following Mild Pediatric Traumatic Brain Injury', *Journal of the International Neuropsychological Society*, 17(05), pp. 886–895. Available at: https://doi.org/10.1017/S1355617711000907.

Babikian, T. and Asarnow, R. (2009) 'Neurocognitive Outcomes and Recovery After Pediatric TBI: Meta-Analytic Review of the Literature', *Neuropsychology*, 23(3), pp. 283–296. Available at: https://doi.org/10.1037/a0015268.

Baliyan, V. *et al.* (2016) 'Diffusion weighted imaging: Technique and applications', *World Journal of Radiology*, 8(9), p. 785. Available at: https://doi.org/10.4329/wjr.v8.i9.785.

Banich, M.T. (2003) 'The divided visual field technique in laterality and interhemispheric integration ', in *Experimental Method in Neuropsychology*. 1st edn, pp. 47–64.

Bashore, T.R. (1981) 'Vocal and manual reaction time estimates of interhemispheric transmission time.', *Psychological bulletin*, 89(2), pp. 352–68. Available at: http://www.ncbi.nlm.nih.gov/pubmed/6262848.

Benavidez, D.A. *et al.* (1999) 'Corpus Callosum Damage and Interhemispherlc Transfer of Information following Closed Head Injury in Children', *Cortex*, 35(3), pp. 315–336. Available at: https://doi.org/10.1016/S0010-9452(08)70803-7.

Berger, A. (2002) ‘How does it work?: Magnetic resonance imaging’, *BMJ*, 324(7328), pp. 35–35. Available at: https://doi.org/10.1136/bmj.324.7328.35.

Blackman, J.A. *et al.* (2003) ‘Brain Imaging as a Predictor of Early Functional Outcome Following Traumatic Brain Injury in Children, Adolescents, and Young Adults’, *Journal of Head Trauma Rehabilitation*, 18(6), pp. 493–503. Available at: https://doi.org/10.1097/00001199-200311000-00003.

Bourne, V.J. (2006) ‘The divided visual field paradigm: Methodological considerations’, *Laterality*, 11(4), pp. 373–393. Available at: https://doi.org/10.1080/13576500600633982.

Bradshaw, J.L. and Perriment, A.D. (1970) ‘Laterality effects and choice reaction time in a unimanual two-finger task’, *Perception & Psychophysics*, 7(3), pp. 185–188. Available at: https://doi.org/10.3758/BF03208654.

Braun, C.M.J., Collin, I. and Mailloux, C. (1997) *The ‘“Poffenberger”’ and ‘ “Dimond”’ Paradigms: Interrelated Approaches to the Study of Interhemispheric Dynamics?*, *BRAIN AND COGNITION*.

Brizzolara, D. *et al.* (1994) ‘Is interhemispheric transfer time related to age? A developmental study’, *Behavioural Brain Research*, 64(1–2), pp. 179–184. Available at: https://doi.org/10.1016/0166-4328(94)90130-9.

Brown, W.S. *et al.* (1999) ‘Bilateral field advantage and evoked potential interhemispheric transmission in commissurotomy and callosal agenesis’, *Neuropsychologia*, 37(10), pp. 1165–1180. Available at: https://doi.org/10.1016/S0028-3932(99)00011-1.

Brown, W.S. and Jeeves, M.A. (1993) ‘Bilateral visual field processing and evoked potential interhemispheric transmission time’, *Neuropsychologia*, 31(12), pp. 1267–1281. Available at: https://doi.org/10.1016/0028-3932(93)90097-J.

Bü ki, A. *et al.* (2000) *Cytochrome c Release and Caspase Activation in Traumatic Axonal Injury*.

Bullock, R. *et al.* (1998) ‘Factors affecting excitatory amino acid release following severe human head injury’, *Journal of Neurosurgery*, 89(4), pp. 507–518. Available at: https://doi.org/10.3171/jns.1998.89.4.0507.

Case, M.E. (2008) ‘Accidental traumatic head injury in infants and young children’, in *Brain Pathology*, pp. 583–589. Available at: https://doi.org/10.1111/j.1750-3639.2008.00203.x.

Catroppa, C. *et al.* (2008) ‘Outcome and predictors of functional recovery 5 years following pediatric traumatic brain injury (TBI)’, *Journal of Pediatric Psychology*, 33(7), pp. 707–718. Available at: https://doi.org/10.1093/jpepsy/jsn006.

Catroppa, C. and Anderson, V. (2006) 'Planning, problem-solving and organizational abilities in children following traumatic brain injury: Intervention techniques', *Pediatric Rehabilitation*, pp. 89–97. Available at: https://doi.org/10.1080/13638490500155458.

Chaumillon, R., Blouin, J. and Guillaume, A. (2018) 'Interhemispheric transfer time asymmetry of visual information depends on eye dominance: An electrophysiological study', *Frontiers in Neuroscience*, 12(FEB). Available at: https://doi.org/10.3389/fnins.2018.00072.

Chevalier, N. *et al.* (2015) 'Myelination is associated with processing speed in early childhood: Preliminary insights', *PLoS ONE*, 10(10). Available at: https://doi.org/10.1371/journal.pone.0139897.

Choi, D. (1987) 'Ionic dependence of glutamate neurotoxicity', *The Journal of Neuroscience*, 7(2), pp. 369–379. Available at: https://doi.org/10.1523/JNEUROSCI.07-02-00369.1987.

Cicero, M.X. and Cross, K.P. (2013) *Predictive Value of Initial Glasgow Coma Scale Score in Pediatric Trauma Patients*. Available at: www.pec-online.com.

Davis, H. *et al.* (1939) *ELECTRICAL REACTIONS OF THE HUMAN BRAIN TO AUDITORY STIMULATION DURING SLEEP*. Available at: www.physiology.org/journal/jn.

Dennis, E.L. *et al.* (2015) 'Callosal function in pediatric traumatic brain injury linked to disrupted white matter integrity', *Journal of Neuroscience*, 35(28), pp. 10202–10211. Available at: https://doi.org/10.1523/JNEUROSCI.1595-15.2015.

Dennis, E.L. *et al.* (2017) 'Diverging volumetric trajectories following pediatric traumatic brain injury', *NeuroImage: Clinical*, 15, pp. 125–135. Available at: https://doi.org/10.1016/j.nicl.2017.03.014.

Dennis, E.L. *et al.* (2018) 'Magnetic resonance spectroscopy of fiber tracts in children with traumatic brain injury: A combined MRS – Diffusion MRI study', *Human Brain Mapping*, 39(9), pp. 3759–3768. Available at: https://doi.org/10.1002/hbm.24209.

Dewan, M.C. *et al.* (2016a) 'Epidemiology of Global Pediatric Traumatic Brain Injury: Qualitative Review', *World Neurosurgery*. Elsevier Inc., pp. 497-509.e1. Available at: https://doi.org/10.1016/j.wneu.2016.03.045.

Dewan, M.C. *et al.* (2016b) 'Epidemiology of Global Pediatric Traumatic Brain Injury: Qualitative Review', *World Neurosurgery*. Elsevier Inc., pp. 497-509.e1. Available at: https://doi.org/10.1016/j.wneu.2016.03.045.

Dismuke, C.E., Walker, R.J. and Egede, L.E. (2015) 'Utilization and Cost of Health Services in Individuals With Traumatic Brain Injury', *Global journal of health science*, pp. 156–169. Available at: https://doi.org/10.5539/gjhs.v7n6p156.

Doezema, D. *et al.* (1991) 'Magnetic resonance imaging in minor head injury', *Annals of Emergency Medicine*, 20(12), pp. 1281–1285. Available at: https://doi.org/10.1016/S0196-0644(05)81065-0.

Ellis, M.U. *et al.* (2016) 'The UCLA study of children with moderate-to-severe traumatic brain injury: Event-related potential measure of interhemispheric transfer time', *Journal of Neurotrauma*, 33(11), pp. 990–996. Available at: https://doi.org/10.1089/neu.2015.4023.

Ewing-Cobbs, L. *et al.* (2016) 'Longitudinal diffusion tensor imaging after pediatric traumatic brain injury: Impact of age at injury and time since injury on pathway integrity', *Human Brain Mapping*, 37(11), pp. 3929–3945. Available at: https://doi.org/10.1002/hbm.23286.

Fabri, M. *et al.* (2014) 'Functional topography of the corpus callosum investigated by DTI and fMRI', *World Journal of Radiology*, 6(12), p. 895. Available at: https://doi.org/10.4329/WJR.V6.I12.895.

Farrell, J.A.D. *et al.* (2007) 'Effects of signal-to-noise ratio on the accuracy and reproducibility of diffusion tensor imaging-derived fractional anisotropy, mean diffusivity, and principal eigenvector measurements at 1.5T', *Journal of Magnetic Resonance Imaging*, 26(3), pp. 756–767. Available at: https://doi.org/10.1002/jmri.21053.

Feldman, H.M. *et al.* (2010) 'Diffusion Tensor Imaging: A Review for Pediatric Researchers and Clinicians', *Journal of Developmental & Behavioral Pediatrics*, 31(4), pp. 346–356. Available at: https://doi.org/10.1097/DBP.0b013e3181dcaa8b.

Figaji, A.A. (2017) 'Anatomical and physiological differences between children and adults relevant to traumatic brain injury and the implications for clinical assessment and care', *Frontiers in Neurology*. Frontiers Media S.A. Available at: https://doi.org/10.3389/fneur.2017.00685.

Friedrich, P. *et al.* (2017) 'Long-term reliability of the visual EEG Poffenberger paradigm', *Behavioural Brain Research*, 330, pp. 85–91. Available at: https://doi.org/10.1016/j.bbr.2017.05.019.

Gagnon, R.F.S.J.S.I. (1998) 'Motor performance following a mild traumatic brain injury in children: an exploratory study', *Brain Injury*, 12(10), pp. 843–853. Available at: https://doi.org/10.1080/026990598122070.

Ghajar, J. (2000) 'Traumatic brain injury', *The Lancet*, 356(9233), pp. 923–929. Available at: https://doi.org/10.1016/S0140-6736(00)02689-1.

Giedd, J.N. *et al.* (1996) *A quantitative MRI study of the corpus callosum in children and adolescents*, *Developmental Brain Research*.

Gorman, S. *et al.* (2017) 'Recovery of Working Memory Following Pediatric Traumatic Brain Injury: A Longitudinal Analysis', *Developmental Neuropsychology*, 42(3), pp. 127–145. Available at: https://doi.org/10.1080/87565641.2017.1315581.

Greve, M.W. and Zink, B.J. (2009) 'Pathophysiology of traumatic brain injury', *Mount Sinai Journal of Medicine*, 76(2), pp. 97–104. Available at: https://doi.org/10.1002/msj.20104.

Haines, K.L. *et al.* (2019) 'Socioeconomic Status Affects Outcomes After Severity-Stratified Traumatic Brain Injury', *Journal of Surgical Research*, 235, pp. 131–140. Available at: https://doi.org/10.1016/j.jss.2018.09.072.

Harvey, L.O. (1978) 'Single representation of the visual midline in humans', *Neuropsychologia*, 16(5), pp. 601–610. Available at: https://doi.org/10.1016/0028-3932(78)90088-X.

Hathcock, J.T. and Stickle, R.L. (1993) 'Principles and Concepts of Computed Tomography', *Veterinary Clinics of North America: Small Animal Practice*, 23(2), pp. 399–415. Available at: https://doi.org/10.1016/S0195-5616(93)50034-7.

Van Heugten, C.M. *et al.* (2006) 'Long-term neuropsychological performance in a cohort of children and adolescents after severe paediatric traumatic brain injury', *Brain Injury*, 20(9), pp. 895–903. Available at: https://doi.org/10.1080/02699050600832015.

Hulkower, M.B. *et al.* (2013) 'A Decade of DTI in Traumatic Brain Injury: 10 Years and 100 Articles Later', *American Journal of Neuroradiology*, 34(11), pp. 2064–2074. Available at: https://doi.org/10.3174/ajnr.A3395.

Ipata, A. *et al.* (1997) 'Interhemispheric transfer of visual information in humans: The role of different callosal channels ', *Archives Italiennes de Biologie* , 135, pp. 169–182.

Jeeves, M.A. and Dixon, N.F. (1970) 'Hemisphere differences in response rates to visual stimuli', *Psychonomic Science*, 20(4), pp. 249–251. Available at: https://doi.org/10.3758/BF03329048.

Johansen-Berg, H. and Behrens, T.E. (2006) 'Just pretty pictures? What diffusion tractography can add in clinical neuroscience', *Current Opinion in Neurology*, 19(4), pp. 379–385. Available at: https://doi.org/10.1097/01.wco.0000236618.82086.01.

Johnson, V.E., Stewart, W. and Smith, D.H. (2013) 'Axonal pathology in traumatic brain injury', *Experimental Neurology*, pp. 35–43. Available at: https://doi.org/10.1016/j.expneurol.2012.01.013.

Jones, T.R. *et al.* (2001) 'Single– versus Multi–Detector Row CT of the Brain: Quality Assessment', *Radiology*, 219(3), pp. 750–755. Available at: https://doi.org/10.1148/radiology.219.3.r01jn47750.

Jonsson, C.A. *et al.* (2013) 'Individual profiles of predictors and their relations to 10 years outcome after childhood traumatic brain injury', *Brain Injury*, 27(7–8), pp. 831–838. Available at: https://doi.org/10.3109/02699052.2013.775493.

Karpiel, I. *et al.* (2021) 'The influence of filters on EEG-ERP testing: Analysis of motor cortex in healthy subjects', *Sensors*, 21(22). Available at: https://doi.org/10.3390/s21227711.

Kaur, P. and Sharma, S. (2018) 'Recent Advances in Pathophysiology of Traumatic Brain Injury', *Current Neuropharmacology*, 16(8), pp. 1224–1238. Available at: https://doi.org/10.2174/1570159X15666170613083606.

Kelly, A.B. *et al.* (1988) 'Head trauma: comparison of MR and CT--experience in 100 patients.', *AJNR. American journal of neuroradiology*, 9(4), pp. 699–708.

Kochunov, P. *et al.* (2012) 'Fractional anisotropy of water diffusion in cerebral white matter across the lifespan', *Neurobiology of Aging*, 33(1), pp. 9–20. Available at: https://doi.org/10.1016/j.neurobiolaging.2010.01.014.

Koessler, L. *et al.* (2009) 'Automated cortical projection of EEG sensors: Anatomical correlation via the international 10-10 system', *NeuroImage*, 46(1), pp. 64–72. Available at: https://doi.org/10.1016/j.neuroimage.2009.02.006.

Koo, T.K. and Li, M.Y. (2016) 'A Guideline of Selecting and Reporting Intraclass Correlation Coefficients for Reliability Research', *Journal of Chiropractic Medicine*, 15(2), pp. 155–163. Available at: https://doi.org/10.1016/j.jcm.2016.02.012.

Kothari, R. *et al.* (2014) *Influence of visual angle on pattern reversal visual evoked potentials*, *of Ophthalmology*.

Koura, S.S. *et al.* (1998) *Relationship between Excitatory Amino Acid Release and Outcome after Severe Human Head Injury*, *Acta Neurochir*.

Ledlow, A., Swanson, J.M. and Kinsbourne, M. (1978) 'Reaction times and evoked potentials as indicators of hemispheric differences for laterally presented name and physical matches.', *Journal of Experimental Psychology: Human Perception and Performance*, 4(3), pp. 440–454. Available at: https://doi.org/10.1037/0096-1523.4.3.440.

Lee, B. and Newberg, A. (2005) 'Neuroimaging in traumatic brain imaging', *NeuroRX*, 2(2), pp. 372–383. Available at: https://doi.org/10.1602/neurorx.2.2.372.

Levin, H.S. *et al.* (1987) 'Magnetic resonance imaging and computerized tomography in relation to the neurobehavioral sequelae of mild and moderate head injuries', *Journal of Neurosurgery*, 66(5), pp. 706–713. Available at: https://doi.org/10.3171/jns.1987.66.5.0706.

Lieh-Lai, M.W. *et al.* (1992) *Limitations of the Glasgow Coma Scale in predicting outcome in children with traumatic brain injury*.

Lifshitz, J. *et al.* (2003) 'Structural and functional damage sustained by mitochondria after traumatic brain injury in the rat: Evidence for differentially sensitive populations in the cortex and hippocampus', *Journal of Cerebral Blood Flow and Metabolism*, 23(2), pp. 219–231. Available at: https://doi.org/10.1097/01.WCB.0000040581.43808.03.

Lipton, M.L. *et al.* (2008) 'Multifocal white matter ultrastructural abnormalities in mild traumatic brain injury with cognitive disability: A voxel-wise analysis of diffusion tensor imaging', *Journal of Neurotrauma*, 25(11), pp. 1335–1342. Available at: https://doi.org/10.1089/neu.2008.0547.

Liu, J. *et al.* (2016) 'Correlation and agreement: overview and clarification of competing concepts and measures', *Shanghai Archives of Psychiatry*, 28(2), pp. 115–120. Available at: https://doi.org/10.11919/j.issn.1002-0829.216045.
St. Louis, E.K. *et al.* (2016) *Electroencephalography (EEG) : an introductory text and atlas of normal and abnormal findings in adults, children, and infants*.

Luck, S.J. (Steven J. (2014) *An introduction to the event-related potential technique*.
Marklund, N. *et al.* (2006) 'Energy metabolic changes in the early post-injury period following traumatic brain injury in rats', *Neurochemical Research*, 31(8), pp. 1085–1093. Available at: https://doi.org/10.1007/s11064-006-9120-0.

Marzi, C.A. (1999) 'The Poffenberger paradigm: a first, simple, behavioural tool to study interhemispheric transmission in humans', *Brain Research Bulletin*, 50(5–6), pp. 421–422. Available at: https://doi.org/10.1016/S0361-9230(99)00174-4.

Mathias, J.L. *et al.* (2004) 'Neuropsychological and information processing performance and its relationship to white matter changes following moderate and severe traumatic brain injury: A preliminary study', *Applied Neuropsychology*, 11(3), pp. 134–152. Available at: https://doi.org/10.1207/s15324826an1103_2.

Mckee, A.C. and Daneshvar, D.H. (2015) *The neuropathology of traumatic brain injury*.

Meissner, T.W. *et al.* (2017) 'Tracking the Functional Development of the Corpus Callosum in Children Using Behavioral and Evoked Potential Interhemispheric Transfer Times', *Developmental Neuropsychology*, 42(3), pp. 172–186. Available at: https://doi.org/10.1080/87565641.2017.1315582.

Mendelsohn, D.B. *et al.* (1992) *Corpus callosum lesions after closed head injury in children: MRI, clinical features and outcome*, *Neuroradiology*.

Menon, D.K. *et al.* (2010) 'Position statement: Definition of traumatic brain injury', *Archives of Physical Medicine and Rehabilitation*. W.B. Saunders, pp. 1637–1640. Available at: https://doi.org/10.1016/j.apmr.2010.05.017.

Meythaler, J.M. *et al.* (2001) 'Current concepts: Diffuse axonal injury-associated traumatic brain injury', *Archives of Physical Medicine and Rehabilitation*, 82(10), pp. 1461–1471. Available at: https://doi.org/10.1053/apmr.2001.25137.

Michinaga, S. and Koyama, Y. (2015) 'Pathogenesis of Brain Edema and Investigation into Anti-Edema Drugs', *International Journal of Molecular Sciences*, 16(12), pp. 9949–9975. Available at: https://doi.org/10.3390/ijms16059949.

Mittl, R.L. *et al.* (1994) 'Prevalence of MR evidence of diffuse axonal injury in patients with mild head injury and normal head CT findings.', *AJNR. American journal of neuroradiology*, 15(8), pp. 1583–9. Available at: http://www.ncbi.nlm.nih.gov/pubmed/7985582.

Mohseni-Bod, H., Drake, J. and Kukreti, V. (2014) 'Management of raised intracranial pressure in children with traumatic brain injury', *Journal of Pediatric Neurosciences*, 9(3), p. 207. Available at: https://doi.org/10.4103/1817-1745.147572.

Muetzel, R.L. *et al.* (2008) 'The development of corpus callosum microstructure and associations with bimanual task performance in healthy adolescents', *NeuroImage*, 39(4), pp. 1918–1925. Available at: https://doi.org/10.1016/j.neuroimage.2007.10.018.

Müller, R. and Büttner, P. (1994) 'A critical discussion of intraclass correlation coefficients', *Statistics in Medicine*, 13(23–24), pp. 2465–2476. Available at: https://doi.org/10.1002/sim.4780132310.

Nell, V. and Brown, D.S.O. (1991) *EPIDEMIOLOGY OF TRAUMATIC JOHANNESBURG-II. MORBIDITY, ETIOLOGY BRAIN INJURY IN MORTALITY AND*, *Soe. Sci. Med*.

Ng, S.Y. and Lee, A.Y.W. (2019) 'Traumatic Brain Injuries: Pathophysiology and Potential Therapeutic Targets', *Frontiers in Cellular Neuroscience*. Frontiers Media S.A. Available at: https://doi.org/10.3389/fncel.2019.00528.

Odom, J.V. *et al.* (2004) *Visual evoked potentials standard (2004) **, *Documenta Ophthalmologica*.

O'Donnell, L.J. and Westin, C.-F. (2011) 'An Introduction to Diffusion Tensor Image Analysis', *Neurosurgery Clinics of North America*, 22(2), pp. 185–196. Available at: https://doi.org/10.1016/j.nec.2010.12.004.

Ogawa, T. *et al.* (1992) 'Comparative Study of Magnetic Resonance and CT Scan Imaging in Cases of Severe Head Injury', in *Neurotraumatology: Progress and Perspectives*. Vienna: Springer Vienna, pp. 8–10. Available at: https://doi.org/10.1007/978-3-7091-9233-7_3.

Okamoto, M. *et al.* (2004) 'Three-dimensional probabilistic anatomical cranio-cerebral correlation via the international 10-20 system oriented for transcranial functional brain mapping', *NeuroImage*, 21(1), pp. 99–111. Available at: https://doi.org/10.1016/j.neuroimage.2003.08.026.

O'Leary, D.S. (1980) 'A Developmental Study of Interhemispheric Transfer in Children Aged Five to Ten', *Child Development*, 51(3), p. 743. Available at: https://doi.org/10.2307/1129460.

Peru, A. *et al.* (2003) 'Temporary and permanent signs of interhemispheric disconnection after traumatic brain injury', *Neuropsychologia*, 41(5), pp. 634–643. Available at: https://doi.org/10.1016/S0028-3932(02)00203-8.

Phillips, N.L. *et al.* (2017) 'Working memory outcomes following traumatic brain injury in children: A systematic review with meta-analysis', *Child Neuropsychology*. Routledge, pp. 26–66. Available at: https://doi.org/10.1080/09297049.2015.1085500.

Pike, B.R. *et al.* (2000) 'Stretch Injury Causes Calpain and Caspase-3 Activation and Necrotic and Apoptotic Cell Death in Septo-Hippocampal Cell Cultures', *Journal of Neurotrauma*, 17(4), pp. 283–298. Available at: https://doi.org/10.1089/neu.2000.17.283.

Pinto, P.S. *et al.* (2012) 'The Unique Features of Traumatic Brain Injury in Children. Review of the Characteristics of the Pediatric Skull and Brain, Mechanisms of Trauma, Patterns of Injury, Complications, and their Imaging Findings-Part 2', *Journal of Neuroimaging*. Available at: https://doi.org/10.1111/j.1552-6569.2011.00690.x.

Popernack, M.L., Gray, N. and Reuter-Rice, K. (2015) 'Moderate-to-Severe Traumatic Brain Injury in Children: Complications and Rehabilitation Strategies', *Journal of Pediatric Health Care*, 29(3), pp. e1–e7. Available at: https://doi.org/10.1016/j.pedhc.2014.09.003.

Poussaint, T.Y. and Moeller, K.K. (2002) 'Imaging of pediatric head trauma', *Neuroimaging Clinics of North America*, 12(2), pp. 271–294. Available at: https://doi.org/10.1016/S1052-5149(02)00005-9.

Povlishock, J.T. (1991) 'Traumatically Induced Axonal Injury: Pathogenesis and Pathobiological Implications', *Brain Pathology*, 2(1), pp. 1–12. Available at: https://doi.org/10.1111/j.1750-3639.1991.tb00050.x.

Prasad, M.R. *et al.* (2002) *Predictors of Outcome following Traumatic Brain Injury in Young Children*, *Pediatr Neurosurg*. Available at: www.karger.comwww.karger.com/journals/pne.

Prigatano, G.P. and Gray, J.A. (2008) 'Predictors of performance on three developmentally sensitive neuropsychological tests in children with and without traumatic brain injury', *Brain Injury*, 22(6), pp. 491–500. Available at: https://doi.org/10.1080/02699050802084902.

Pudenz, R.H. and Shelden, C.H. (1946) 'The Lucite Calvarium—A Method for Direct Observation of the Brain', *Journal of Neurosurgery*, 3(6), pp. 487–505. Available at: https://doi.org/10.3171/jns.1946.3.6.0487.

Ratinckx, E. (1997) 'Age and interhemispheric transfer time: a failure to replicate', *Behavioural Brain Research*, 86(2), pp. 161–164. Available at: https://doi.org/10.1016/S0166-4328(96)02261-9.

Von Reyn, C.R. *et al.* (2012) 'Mechanisms of calpain mediated proteolysis of voltage gated sodium channel α-subunits following in vitro dynamic stretch injury', *Journal of Neurochemistry*, 121(5), pp. 793–805. Available at: https://doi.org/10.1111/j.1471-4159.2012.07735.x.

Robertson, C.L., Saraswati, M. and Fiskum, G. (2007) 'Mitochondrial dysfunction early after traumatic brain injury in immature rats', *Journal of Neurochemistry*, 101(5), pp. 1248–1257. Available at: https://doi.org/10.1111/j.1471-4159.2007.04489.x.

Saron, C.D. and Davidson, R.J. (1989) *Visual Evoked Potential Measures of Interhemispheric Transfer Time in Humans*, *Behavioral Neuroscience*.

Scharinger, C., Schüler, A. and Gerjets, P. (2020) 'Using eye-tracking and EEG to study the mental processing demands during learning of text-picture combinations', *International Journal of Psychophysiology*, 158, pp. 201–214. Available at: https://doi.org/10.1016/j.ijpsycho.2020.09.014.

Schrieff, L.E. *et al.* (2013) 'Demographic profile of severe traumatic brain injury admissions to Red Cross War Memorial Children's Hospital, 2006-2011', *South African Medical Journal*, 103(9), pp. 616–620. Available at: https://doi.org/10.7196/SAMJ.7137.

Scrivener, C.L. and Reader, A.T. (2022) 'Variability of EEG electrode positions and their underlying brain regions: visualizing gel artifacts from a simultaneous EEG-fMRI dataset', *Brain and Behavior*, 12(2). Available at: https://doi.org/10.1002/brb3.2476.

Seghier, M.L. (2013) 'The angular gyrus: Multiple functions and multiple subdivisions', *Neuroscientist*, pp. 43–61. Available at: https://doi.org/10.1177/1073858412440596.
Shobhit Jain, A. and Iverson Affiliations, L.M. (2022) *Glasgow Coma Scale Continuing Education Activity*. Available at: https://www.ncbi.nlm.nih.gov/books/NBK513298/?report=printable.

Singh, I.N. *et al.* (2006) 'Time course of post-traumatic mitochondrial oxidative damage and dysfunction in a mouse model of focal traumatic brain injury: Implications for neuroprotective

therapy', *Journal of Cerebral Blood Flow and Metabolism*, 26(11), pp. 1407–1418. Available at: https://doi.org/10.1038/sj.jcbfm.9600297.

Sinson, G. *et al.* (2001) 'Magnetization transfer imaging and proton MR spectroscopy in the evaluation of axonal injury: correlation with clinical outcome after traumatic brain injury.', *AJNR. American journal of neuroradiology*, 22(1), pp. 143–51.

Smith, L.G.F. *et al.* (2019) 'Advanced neuroimaging in traumatic brain injury: An overview', *Neurosurgical Focus*, 47(6). Available at: https://doi.org/10.3171/2019.9.FOCUS19652.

Song, J. *et al.* (2015) 'DTI measures track and predict motor function outcomes in stroke rehabilitation utilizing BCI technology', *Frontiers in Human Neuroscience*, 9. Available at: https://doi.org/10.3389/fnhum.2015.00195.

Strangman, G.E. *et al.* (2012) 'Fractional anisotropy helps predicts memory rehabilitation outcome after traumatic brain injury', *NeuroRehabilitation*, 31(3), pp. 295–310. Available at: https://doi.org/10.3233/NRE-2012-0797.

Suskauer, S.J. and Huisman, T.A.G.M. (2009) 'Neuroimaging in pediatric traumatic brain injury: Current and future predictors of functional outcome', *Developmental Disabilities Research Reviews*, 15(2), pp. 117–123. Available at: https://doi.org/10.1002/ddrr.62.

Tanaka-Arakawa, M.M. *et al.* (2015) 'Developmental changes in the corpus callosum from infancy to early adulthood: A structural magnetic resonance imaging study', *PLoS ONE*, 10(3). Available at: https://doi.org/10.1371/journal.pone.0118760.

Tang, P.H. and Lim, C.C.T. (2009) 'Imaging of accidental paediatric head trauma', *Pediatric Radiology*, pp. 438–446. Available at: https://doi.org/10.1007/s00247-008-1083-7.

Taylor, H.G. and Alden, J. (1997) 'Age-related differences in outcomes following childhood brain insults: an introduction and overview.', *Journal of the International Neuropsychological Society : JINS*, 3(6), pp. 555–67.

Thurman, D.J. (2016) 'The epidemiology of traumatic brain injury in children and youths: A review of research since 1990', *Journal of Child Neurology*. SAGE Publications Inc., pp. 20–27. Available at: https://doi.org/10.1177/0883073814544363.

Tzourio-Mazoyer, N. (2016) 'Intra- and inter-hemispheric connectivity supporting hemispheric specialization', in *Research and Perspectives in Neurosciences*. Springer Verlag, pp. 129–146. Available at: https://doi.org/10.1007/978-3-319-27777-6_9.

Unterberg, A.W. *et al.* (2004) 'Edema and brain trauma', *Neuroscience*, 129(4), pp. 1019–1027. Available at: https://doi.org/10.1016/j.neuroscience.2004.06.046.

Wakana, S. *et al.* (2004) ‘Fiber Tract–based Atlas of Human White Matter Anatomy’, *Radiology*, 230(1), pp. 77–87. Available at: https://doi.org/10.1148/radiol.2301021640.
Weber, B. *et al.* (2005) ‘Attention and Interhemispheric Transfer: A Behavioral and fMRI Study’, *Journal of Cognitive Neuroscience*, 17(1), pp. 113–123. Available at: https://doi.org/10.1162/0898929052880002.

Webster, J., Taylor, A. and Balchin, R. (2015) ‘Traumatic brain injury, the hidden pandemic: A focused response to family and patient experiences and needs’, *South African Medical Journal*, 105(3), pp. 195–198. Available at: https://doi.org/10.7196/SAMJ.9014.

Westerhausen, R. *et al.* (2006) ‘Interhemispheric transfer time and structural properties of the corpus callosum’, *Neuroscience Letters*, 409(2), pp. 140–145. Available at: https://doi.org/10.1016/j.neulet.2006.09.028.

Wilde, E.A. *et al.* (2006) ‘Vulnerability of the Anterior Commissure in Moderate to Severe Pediatric Traumatic Brain Injury’, *J Child Neurol*, 21, pp. 769–776. Available at: https://doi.org/10.2310/7010.2006.00152.

Woodman, G.F. (2010) ‘A brief introduction to the use of event-related potentials in studies of perception and attention’, *Attention, Perception & Psychophysics*, 72(8), pp. 2031–2046. Available at: https://doi.org/10.3758/app.72.8.2031.

Wu, T.C. *et al.* (2011) ‘Longitudinal Changes in the Corpus Callosum following Pediatric Traumatic Brain Injury’, *Developmental Neuroscience*, 32(5–6), pp. 361–373. Available at: https://doi.org/10.1159/000317058.